Available online at www.sciencedirect.com

ScienceDirect

Geochimica et Cosmochimica Acta 138 (2014) 32–56

Geochimica et Cosmochimica Acta

www.elsevier.com/locate/gca

Re–Os geochronology and Os isotope fingerprinting of petroleum sourced from a Type I lacustrine kerogen: Insights from the natural Green River petroleum system in the Uinta Basin and hydrous pyrolysis experiments

Vivien M. Cumming [a,b,*], David Selby [a], Paul G. Lillis [c], Michael D. Lewan [c]

[a] Department of Earth Sciences, Durham University, Durham DH1 3LE, UK
[b] Department of Earth and Planetary Sciences, Harvard University, 20 Oxford Street, Cambridge, MA 02138, USA
[c] U.S. Geological Survey, P.O. Box 25046, MS977, Denver Federal Center, Denver, CO 80225, USA

Received 13 July 2013; accepted in revised form 11 April 2014; available online 21 April 2014

Abstract

Rhenium–osmium (Re–Os) geochronology of marine petroleum systems has allowed the determination of the depositional age of source rocks as well as the timing of petroleum generation. In addition, Os isotopes have been applied as a fingerprinting tool to correlate oil to its source unit. To date, only classic marine petroleum systems have been studied. Here we present Re–Os geochronology and Os isotope fingerprinting of different petroleum phases (oils, tar sands and gilsonite) derived from the lacustrine Green River petroleum system in the Uinta Basin, USA. In addition we use an experimental approach, hydrous pyrolysis experiments, to compare to the Re–Os data of naturally generated petroleum in order to further understand the mechanisms of Re and Os transfer to petroleum.

The Re–Os geochronology of petroleum from the lacustrine Green River petroleum system (19 ± 14 Ma – all petroleum phases) broadly agrees with previous petroleum generation basin models (~25 Ma) suggesting that Re–Os geochronology of variable petroleum phases derived from lacustrine Type I kerogen has similar systematics to Type II kerogen (e.g., Selby and Creaser, 2005a,b; Finlay et al., 2010). However, the large uncertainties (over 100% in some cases) produced for the petroleum Re–Os geochronology are a result of multiple generation events occurring through a ~3000-m thick source unit that creates a mixture of initial Os isotope compositions in the produced petroleum phases. The $^{187}Os/^{188}Os$ values for the petroleum and source rocks at the time of oil generation vary from 1.4 to 1.9, with the mode at ~1.6. Oil-to-source correlation using Os isotopes is consistent with previous correlation studies in the Green River petroleum system, and illustrates the potential utility of Os isotopes to characterize the spatial variations within a petroleum system.

Hydrous pyrolysis experiments on the Green River Formation source rocks show that Re and Os transfer are mimicking the natural system. This transfer from source to bitumen to oil does not affect source rock Re–Os systematics or Os isotopic compositions. This confirms that Os isotope compositions are transferred intact from source to petroleum during petroleum generation and can be used as a powerful correlation tool. These experiments further confirm that Re–Os systematics in source rocks are not adversely affected by petroleum maturation. Overall this study illustrates that the Re–Os petroleum geochronometer and Os isotope fingerprinting tools can be used on a wide range of petroleum types sourced from variable kerogen types.

* Corresponding author at: Department of Earth and Planetary Sciences, Harvard University, 20 Oxford Street, Cambridge, MA 02138, USA. Tel.: +1 (617) 495 2351; fax: +1 (617) 495 8839.
E-mail address: vcumming@g.harvard.edu (V.M. Cumming).

http://dx.doi.org/10.1016/j.gca.2014.04.016
0016-7037/

1. INTRODUCTION

The majority of large oil discoveries are sourced from marine shales associated with major ocean anoxic events of the Jurassic and Cretaceous (Klemme and Ulmishek, 1991). Such large discoveries are becoming increasingly rare and thus there is a need to understand the mechanisms of smaller petroleum systems and more accurately trace oils to their source in order to improve migration pathway models and reserve calculations (Hindle, 1997). A common problem for petroleum exploration surrounds understanding the spatial and temporal controls on petroleum formation. Establishing the timing of petroleum generation has, to date, mainly been carried out through the use of basin modelling, often with poorly constrained parameters (e.g., Anders et al., 1992; Bredehoeft et al., 1994; Scotchman et al., 2006; Higley et al., 2009). Therefore, knowing the absolute age of petroleum generation provides vital information and controls on the understanding of a petroleum system framework.

The application of the rhenium–osmium (Re–Os) geochronometer to marine petroleum systems has permitted the determination of source rock depositional ages (e.g., Cohen et al., 1999; Creaser et al., 2002; Selby et al., 2005; Kendall et al., 2009; Xu et al., 2009; Rooney et al., 2010) and the timing of petroleum generation (Selby et al., 2005; Selby and Creaser, 2005a; Finlay et al., 2011). Furthermore, Os isotopes have been successfully used in marine basins to correlate oils to their source rocks (Finlay et al., 2012). Traditionally, oil-source rock correlations use organic geochemical analysis of light hydrocarbon fractions (e.g., biomarkers), however common processes such as biodegradation preferentially remove light hydrocarbons from petroleum and therefore, oil-to-source fingerprinting techniques can be compromised. Petroleum Re–Os geochronology and Os isotope fingerprinting, however, utilize the biodegradation-resistant asphaltene fraction of oil (Selby et al., 2007). The Os isotope fingerprinting tool uses the initial $^{187}Os/^{188}Os$ composition (Os_i) of petroleum which reflects the source rock at the time of petroleum generation (Os_g) providing a novel inorganic oil-source correlation technique (Selby et al., 2007; Finlay et al., 2011, 2012). As a result, inorganic geochemistry provides a correlation tool where traditional organic methods may be hampered by biodegradation (Finlay et al., 2012).

Despite the promising success of Re–Os petroleum geochronology and Os isotope fingerprinting in marine basins, there remains little knowledge of the mechanism of Re and Os transfer from source rocks to oils (Selby et al., 2007; Rooney et al., 2012). A hydrous pyrolysis study of the Permian Phosphoria (Type II-S kerogen) and Jurassic Staffin Formations (Type III kerogen) involved artificial maturation of the source rocks in order to assess transfer of Re and Os from source rock to oil (Rooney et al., 2012). These experiments demonstrated that Re–Os systematics in the source rock were undisturbed during petroleum maturation as previously suggested in the natural system (Creaser et al., 2002; Selby and Creaser, 2005a). However, there was limited Re and Os in the oils produced since the kinetic parameters needed for transfer were not attained in these artificial experiments (Rooney et al., 2012). The bitumen produced contained Re and Os and it was found that during petroleum generation the Os isotope composition of the source is transferred to the bitumen. This behaviour has been noted in previous studies and so provides further evidence that Os isotopes can be used as an oil-source correlation tool, supporting data derived from natural petroleum system studies (Selby et al., 2005, 2007; Selby and Creaser, 2005a; Finlay et al., 2012). However, given that the Re–Os petroleum geochronology and Os isotope fingerprinting tools have only been assessed in marine petroleum systems sourced from Type II and Type II-S kerogens (Selby et al., 2005; Selby and Creaser, 2005a; Finlay et al., 2011, 2012), there is need for further assessment and understanding of Re–Os systematics during petroleum generation as well as in variable basin types in order to widen the applications of Re–Os petroleum geochronology and Os isotope fingerprinting.

The Green River petroleum system in the Uinta Basin (Fig. 1) contains Type I lacustrine source rocks that have produced several different forms of petroleum (oil, gas, tar sands and gilsonite) that are both biodegraded and non-biodegraded (Tissot et al., 1978; Anders et al., 1992; Fouch et al., 1994; Katz, 1995; Ruble et al., 2001). The Green River petroleum system therefore provides the ability to test whether Re–Os geochronology and Os isotope fingerprinting can be applied to different petroleum phases,

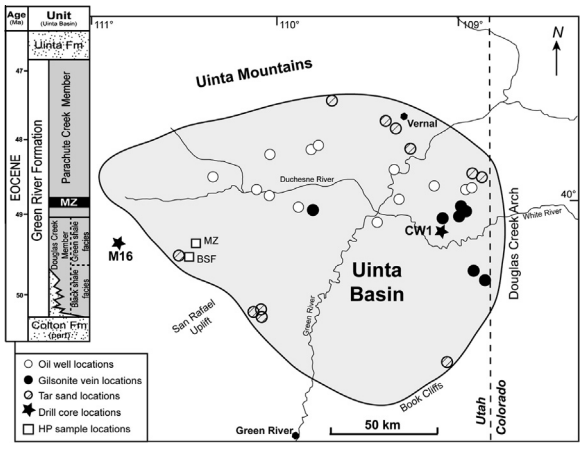

Fig. 1. Map of the Uinta Basin illustrating the location of the sampled petroleum and the source rocks sampled from two drill cores; Marsing 16 (M16; 39°57′1.4904″N, 111°1′37.527″W) and Coyote Wash 1 (CW1; 40°1′22.224″N, 109°18′38.4834″W). The CW1 core is located in the central depocentre of an asymmetric basin structure, while the M16 core is on the flank of this structure and has not seen significant burial. The outcrop samples used for the hydrous pyrolysis (HP) experiments are also shown, the Mahogany zone (MZ; 930923–8; 39°53′12″N, 110°44′58″W) and black shale facies (BSF; 930922-1; 39°50′09″N, 110°47′05″W). Schematic stratigraphy of the Green River Formation is provided in the inset. This shows the intertonguing nature of the basal sandstones with the Douglas Creek Member. The Douglas Creek Member is split into the black shale and green shale facies after Ruble et al. (2001). Ages of the stratigraphy are based on chronostratigraphy of Smith et al. (2008).

biodegraded and non-biodegraded, and to petroleum systems derived from a Type I lacustrine kerogen. Here we explore the capabilities of Re–Os geochronology and Os isotope fingerprinting on the Green River petroleum system to further establish the behaviour of these geochemical systems and widen their application to poorly constrained or non-traditional petroleum systems. In addition we use hydrous pyrolysis experiments to further delineate the nature of Re and Os transfer to oil in particular with Type I lacustrine kerogen. These data permit valuable comparison to a natural system and provide an experimental approach on the same source rock in order to understand Re–Os systematics within petroleum systems.

2. GEOLOGICAL SETTING

The Green River petroleum system of the Uinta Basin in northwest Utah receives considerable attention as it has produced more than 500 million barrels oil, has greater than 12 billion barrels oil inferred in tar sand deposits, and an estimated 1 trillion barrels of recoverable oil in oil shale and solid bitumen deposits (Fig. 1; Hunt, 1963; Anders et al., 1992; Fouch et al., 1994; Ruble et al., 2001; Dyni, 2006). The source rock for this petroleum system is the Eocene Green River Formation; a classic model for lacustrine source rock deposition and petroleum generation from these types of source rock facies (Ruble et al., 2001). The unit exhibits variable organic enrichment (0.2–33.7 wt.% total organic carbon [TOC]; Katz, 1995) and is the common reference type for a typical Type I kerogen (Vandenbroucke and Largeau, 2007).

The Green River Formation was deposited in three large continental basins named the Uinta, Piceance, and Greater Green River Basins located in Colorado, Wyoming and Utah, USA. The Uinta Basin is the focus of this study as it contains a mature petroleum system. The basins formed east of the thin-skinned Sevier orogenic belt, and are separated by Laramide basement-cored uplifts, geometry of which is controlled by Precambrian and late Palaeozoic structures (Johnson, 1992). The depocentres were occupied by two large lakes that covered an area of 65,000 km^2 during a period of temperate to subtropical climate throughout the early to middle Eocene (Dyni, 2006; Smith et al., 2008). The Green River Formation was deposited in freshwater to hypersaline lakes and lake level fluctuations allowed thick packages (~3000 m) of organic-rich carbonaceous shales and oil shales interbedded with fluvial clastics to be deposited (Keighley et al., 2003; Pietras and Carroll, 2006). Sedimentary facies within the Green River Formation can be divided into fluvio-lacustrine, fluctuating profundal, and evaporative facies (Carroll and Bohacs, 1999, 2001; Bohacs et al., 2000). The most important members of the Green River Formation in terms of source rocks are the Douglas Creek Member and Parachute Creek Member, found predominantly in the Uinta Basin. The Douglas Creek Member was deposited initially as lake levels rose and represents fluctuating profundal deposition (Bradley, 1931; Tuttle and Goldhaber, 1993; Carroll and Bohacs, 2001). Here organic-rich units of the informally named black shale facies were deposited that are considered by some to be the only units to have generated oil (Remy, 1992; Katz, 1995; Ruble et al., 2001). The maximum extent of the lake occurred during deposition of the overlying Parachute Creek Member, and was coincident with deposition of the most organic-rich oils shales (>30 wt.% TOC) in the Mahogany zone (Bradley, 1931; Tuttle and Goldhaber, 1993; Smith et al., 2008). Despite the high TOC, this unit is not considered to be a significant source of petroleum due to insufficient burial, thus it is a target for oil shale extraction (Ruble et al., 2001; Dyni, 2006). Due to a lack of detailed biostratigraphy in lacustrine records, the Green River Formation has been dated using predominantly ^{40}Ar–^{39}Ar and U–Pb geochronology of interbedded tuffs as well as Re–Os dating of the source rock itself, with deposition constrained from ~52 to ~44 Ma (Smith et al., 2008, 2010; Cumming et al., 2012).

The Green River Formation source rocks are deposited throughout the area, but have only been sufficiently buried for oil and gas generation in the central-northeast portion of the Uinta Basin (Tissot et al., 1978; Ruble et al., 2001). The thickness and nature of the lacustrine sedimentary facies suggests that the Green River Formation contains both the source rock for this petroleum system, and most of the reservoir and seal rocks (Fouch et al., 1994). The erosional remnant of the Uinta Basin crops out along the southern limb of the basinal syncline, dipping <5° to the north (Keighley et al., 2003). Several oil fields (e.g., Altamont, Bluebell and Duchesne) produce from lenticular lacustrine sandstone and carbonate reservoirs, with alluvial deposits acting as seals stratigraphically trapping oil in downdip reservoirs (Fouch et al., 1994). Migration distance for the oils is ⩽100 km. The tar sands are surface expressions of oil that have migrated up structural dip through fluvio-lacustrine facies connected to the deeper oil fields. Most of the accumulations are associated with source rocks with vitrinite reflectance >0.5% R_m (0.5–0.7% R_m = moderately mature; Anders et al., 1992; Fouch et al., 1994). Early oil-generation models suggest that generation began at the base of the Green River Formation around 40 Ma (only ~10 Myr after deposition) at a depth of 3350 m, with peak-oil generation in this lower stratigraphy probably occurring during maximum burial (40–30 Ma; Fouch et al., 1994). Generation then decreased from 30 Ma to the present day, and the zone of generation has risen stratigraphically through time. It is also suggested that the Mahogany zone began petroleum generation ~25 Ma and that generation is probably still ongoing (Fouch et al., 1994). Ruble et al. (2001) more recently proposed, by using hydrous pyrolysis kinetic models, that petroleum generation only began in the lower part of the Green River Formation ~25 Ma and is ongoing to the present day. While the Mahogany zone has yet to reach peak-oil generation, there is likely limited generation from this source unit.

Although this is a relatively self-contained petroleum system in the Uinta Basin with the Green River Formation providing both source and reservoir (Fouch et al., 1994), the source unit is over 3000 m thick in places creating ambiguity on the exact units generating oil (Anders et al., 1992). Additionally, oil-source rock correlation in these settings is

complicated as multifaceted lacustrine facies can obscure maturity relationships usually distinguished by biomarkers (Ruble et al., 2001). This lacustrine basin therefore provides an ideal petroleum system to test the Re–Os petroleum geochronometer and Os isotope oil-source correlation tool on more diverse petroleum systems in order to extend their applicability.

3. ANALYTICAL METHODOLOGY

3.1. Samples and sample preparation

3.1.1. Oils

Oils were obtained from the U.S. Geological Survey oil library, Denver, Colorado for Re–Os analysis. Well locations (Fig. 1) with well names, oil fields, reservoir stratigraphic unit, and organic geochemical properties of each sample are given in Table 1. The sample set provides a representation of oils from fields across the entire Uinta Basin. Two oil types are recognised in the Uinta Basin, Green River A (GRA; the most common) and Green River B (GRB), which are defined based on organic geochemical parameters and are interpreted to have been sourced from the lower black shale facies of the Douglas Creek Member and the Mahogany zone, respectively (Lillis et al., 2003). Source identification is based on the presence of β-carotane in the GRB oils, which is derived from the Mahogany source facies (Fig. 2).

The asphaltene fraction of the oil is utilised for the Re–Os analyses because it contains >90% of the Re and Os within the oil and possesses Re–Os isotopic compositions identical to and more precise than whole-oil analysis (Selby et al., 2007). Asphaltene was precipitated from the Green River oils using *n*-heptane (c.f. Selby et al., 2007). This process involved 1 g of oil being thoroughly mixed in 40 ml of *n*-heptane in a 60 ml glass vial and then agitated for ~12 h. The contents of the vial were then centrifuged at 4000 rpm for 5 minutes to allow complete separation of the insoluble asphaltene and soluble maltene fractions. The asphaltene was dried on a hot plate at ~60 °C and then used for Re–Os analysis.

3.1.2. Tar sands

Tar sands were collected from outcrop throughout the Uinta Basin giving a wide representation of the instances of oil that has migrated updip from deeper oils fields. Location and names of deposits are reported in Table 1 and Fig. 1. Approximately ~500 g of tar sand was collected to ensure enough oil could be extracted from it for Re–Os analysis. The tar sands are heavily biodegraded oil accumulations the source of which is thought to be the same as the GRA oils (Fouch et al., 1994; Ruble et al., 2001; Lillis et al., 2003).

Oil is separated from the Green River tar sands using a method modified from Selby et al. (2005). Approximately 1 g of tar sand was rinsed in ~1/2 ml of $CHCl_3$ and then decanted into a 15 ml centrifuge tube, and repeated until the $CHCl_3$ remained clear. The $CHCl_3$ and oil solution was then centrifuged to separate any suspended sediment from the solution. The $CHCl_3$ in the decanted solution was evaporated at ~60 °C on a hot plate leaving the oil remaining. Tar sands are heavily biodegraded and are therefore naturally enriched in asphaltene (Evans et al., 1971), with the average for some of the Green River tar sands being ~34 wt.% (Table 1), rendering separation of asphaltenes for Re–Os analysis unnecessary (c.f. Selby and Creaser, 2005a).

3.1.3. Gilsonite

Gilsonite is one of several types of solid bitumen deposits found in the Uinta Basin which include; ozocerite, albertite, tabbyite and wurtzilite (Ruble and Philp, 1991), with gilsonite being the most abundant (Verbeek and Grout, 1992). It crops out in northwest trending vertical fractures up to 5 m thick within the middle and upper parts of the Green River Formation (Cashion, 1967; Anders et al., 1992; Verbeek and Grout, 1992). The method of formation is not fully understood with suggestions of oil reservoirs penetrated by fractures allowing oil to migrate up the fractures and then solidify from inspissation or metamorphosis (Tetting, 1984). Other suggestions are that they are derived from early bitumen generation processes causing overpressured source beds to initiate hydraulic fracturing (Verbeek and Grout, 1992). The fractures containing gilsonite originate in the lacustrine facies of the Green River Formation, in particular the Mahogany zone, leading to suggestions of the Mahogany zone as the source where early maturity generation occurred and liquid petroleum migrated into tensile fractures created during uplift (Hunt et al., 1954; Hunt, 1963) or where overpressure allowed hydraulic fracturing of the rock to produce the veins (Verbeek and Grout, 1992). The Mahogany zone was further supported as the source based on infrared spectroscopy (Hunt et al., 1954) and carbon isotope and biomarker compositions (Ruble et al., 1994; Schoell et al., 1994).

Several gilsonite samples were collected from outcrops of different fracture systems throughout the Uinta Basin (Table 1, Fig. 1). Approximately 50–100 g samples were collected and then crushed with no metal contact for analysis. Gilsonite, although only moderately biodegraded (Fig. 2; Ruble et al., 1994), is naturally enriched in asphaltene (the average for two Green River samples is ~78.5 wt.%; Table 1) and so separation of asphaltene is unnecessary for Re–Os analysis.

3.1.4. Source rocks

Three Green River Formation source units from the Uinta Basin have previously been analysed for Re–Os isotopes, with the data presented in Table 2 (Cumming et al., 2012). The units were sampled from two cores held at the U.S. Geological Survey Core Research Center, Denver, Colorado; Coyote Wash 1 (CW1) in the central depocentre and Marsing 16 (M16) at the southwest edge of the Basin (Fig. 1). The Douglas Creek Member (TOC = 2.67–24.70 wt.%, T_{max} = 434–448 °C; Cumming et al., 2012) was sampled from both cores and the Mahogany zone (TOC = 9.39–28.15 wt.%, T_{max} = 432–445 °C; Cumming et al., 2012) was sampled from the CW1 core. Additional analyses were performed to assess the spread of Os isotopic compositions across 30–50 m of each unit

Table 1
Sample information for the oils, tar sands and gilsonites.

Sample	Hydrocarbon	Field/deposit	Well name	Stratigraphic unit	Latitude	Longitude	β-carotane	Oil type	Asph (%)	Biodegradation
GR2268	Oil – USGS	Bluebell	Lamicq 2-6B1	Green River/Wasatch	40.335	−110.034	Trace	GRA	4.78	No (0)
GR2266	Oil – USGS	Coyote Basin	Coyote Basin 21-7	Wasatch	40.143	−109.146	0	GRA	8.00	No (0)
GR2232	Oil – USGS	Coyote Basin	E. Red Wash 1-5	Green River	40.153	−109.126	0	GRA	7.37	No (0)
GR2239	Oil – USGS	Duchesne	Ute. Tribal 6-16 D	Green River	40.139	−110.344	Trace	GRA	8.88	No (0)
GR2269	Oil – USGS	Horseshoe Bend	Federal 33-7 L	Green River	40.253	−109.566	+	GRA	7.24	No (0)
GR2264	Oil – USGS	Monument Butte	Federal 23-34B	Green River	40.072	−110.107	+	GRA	5.95	No (0)
GR2242	Oil – USGS	Natural Buttes	Natural Duck 4-21	Green River	40.026	−109.665	+	GRA	7.94	No (0)
GR2267	Oil – USGS	Wonsits Valley	WVU 133 & 71	Green River	40.118	−109.543	+	GRA	6.49	No (0)
GR2259	Oil – USGS	Altamont	Myrin Ranch 1-13 B4	Wasatch	40.312	−110.278	+	GRA	7.09	No (0)
GR2114	Oil – USGS	Sulphur Creek	Govt. 29-3	Wasatch	39.845	−108.414	++	GRA	9.77	No (0)
GRB-827	Oil – USGS	Bluebell	L L Pack 1-33A1	Green River	40.352	−110.004	++	GRB	18.50	No (0)
GRB-3885	Oil – USGS	Duchesne	Ute-Tribal 8	Green River	40.139	−110.348	++++	GRB	19.00	Slightly (1)
GRB-1602	Oil – USGS	Duchesne	Willis Moon 1	Green River	40.130	−110.277	++++	GRB	14.06	Slightly (1)
GRB-847	Oil – USGS	Blacktail Ridge	Ute Tribal 2/22-18	Green River	40.221	−110.607	++++	GRB	2.20	No (0)
GRB-824	Oil – USGS	Red Wash	Red Wash 120 23-28B	Green River	40.179	−109.334	++	GRB	1.65	No (0)
VC07-10	Gilsonite – USGS	Bonanaza vein	–	Uinta Formation	40.036	−109.229	–	GRB	–	–
VC05-10	Gilsonite – USGS	Cowboy vein	–	Uinta Formation	40.073	−109.220	–	GRB	–	–
VC06-10	Gilsonite – USGS	Rainbow vein	–	Upper Parachute Creek	39.822	−109.154	–	GRB	–	–
VC08-10	Gilsonite – USGS	Dragon mine	–	Lower Douglas Creek	39.775	−109.085	–	GRB	–	–
VC09-10	Gilsonite – USGS	CW1 core vein	–	Mahogany zone	40.023	−109.311	–	GRB	–	–
VC44-10	Gilsonite – TR	Little Emma vein	–	–	–	–	–	GRB	–	–
VC45-10	Gilsonite – TR	Bonanza	–	–	–	–	–	GRB	–	–
VC46-10	Gilsonite – TR	Independant	–	–	–	–	–	GRB	–	–
VC47-10	Gilsonite – TR	Cowboy	–	–	–	–	–	GRB	–	–
VC12-10	Gilsonite – field	Cowboy/Bonanza	–	Uinta Formation	40.068	−109.201	++++	GRB	83.89	Moderate (4)
VC16-10	Gilsonite – field	Pariette Bench	–	Uinta Formation	40.071	−110.028	++++	GRB	73.19	Moderate (4)
VC34-10	Gilsonite – UCRC	Bonanza	–	–	–	–	–	GRB	–	–
VC03-10	Tar Sand – USGS	Asphalt Ridge	–	–	40.447	−109.616	0	GRA	–	Heavy (5–6)
VC02-10	Tar Sand – USGS	Sunnyside	Amoco A-22	–	39.630	−110.310	0	GRA	–	Heavy (5–6)
VC01-10	Tar Sand – USGS	Raven ridge	–	Upper Douglas Creek	40.206	−109.098	++	GRA	–	Heavy (5–6)
VC04-10	Tar Sand – USGS	PR Springs	–	Upper Douglas Creek	39.439	−109.292	+	GRA	–	Heavy (5–6)
VC35-10	Tar Sand – UCRC	PR Springs	PRS-3	Upper Douglas Creek	–	–	–	GRA	–	–
VC10-10	Tar Sand – field	White Rocks	–	Navajo Sandstone	40.569	−109.918	Trace	GRA	15.85	Heavy (5–6)
VC11-10	Tar Sand – field	Raven Ridge	–	Parachute Creek	40.225	−109.128	Trace	GRA	26.80	Heavy (5–6)
VC14-10	Tar Sand – field	Asphalt Ridge	–	Duschesne River	40.336	−109.485	Trace	GRA	36.95	Heavy (5–6)
VC15-10	Tar Sand – field	Asphalt Ridge	–	Duschesne River	40.416	−109.583	++	GRA	45.63	Severe (7+)
VC20-10	Tar Sand – field	Sunnyside	–	Green River – lower	39.636	−110.348	Trace	GRA	14.01	(6–7)
VC25-10	Tar Sand – field	Sunnyside	–	Green River – lower	39.636	−110.350	Trace	GRA	27.22	(6–7)
VC32-10	Tar Sand – field	Sunnyside	–	Green River – lower	39.635	−110.347	Trace	GRA	21.22	(6–7)
VC33-10	Tar Sand – field	Willow Creek	–	Green River – lower	39.844	−110.774	++	GRA	84.20	Severe (7+)

(–) no data for these samples.
USGS = U.S. Geological Survey.
TR = donated by Tim Ruble, Weatherford Laboratories.
UCRC = Utah Core Research Centre.
β-carotane estimates based on gas chromatograms of USGS.
0 = none; no β-carotane peak.
tr = trace; very small peak elutes at the correct time.
+ = minor; β-carotane peak height about the same as adjacent *n*-alkanes (*n*-C 36–37).
++ = moderate; β-carotane peak height bigger than adjacent peak (*n*-C 30+).
+++ = moderately high.
++++ = high; carotane peak high bigger that most, if not all *n*-alkanes.
Oil type based on β-carotane (Lillis et al., 2003).
Asph = percentage asphaltene content derived from asphaltene extractions (oils) or USGS analysis.
Biodegradation scale is zero to ten (Peters et al., 2005).

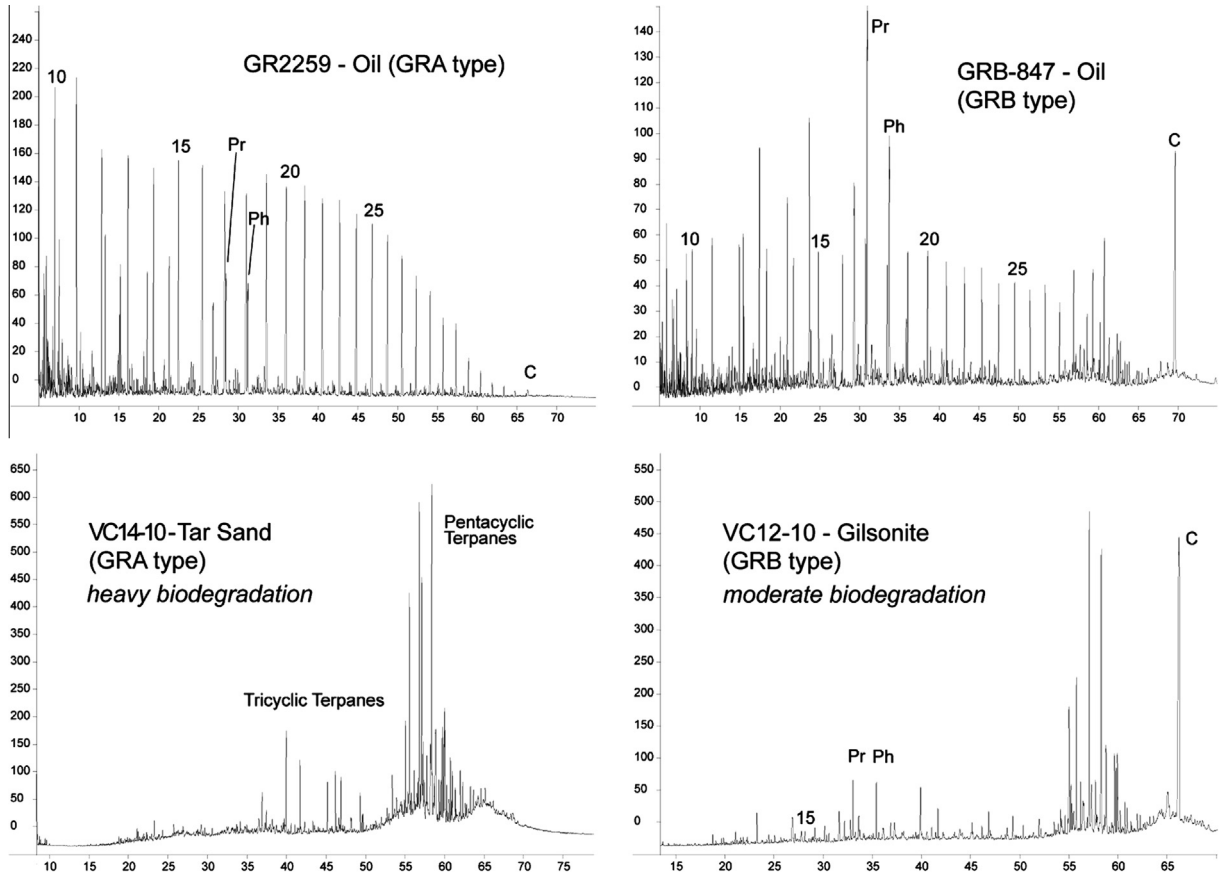

Fig. 2. Gas chromatograms of the saturated petroleum fraction of selected oils, tar sands, and gilsonite from the Uinta Basin, Utah, showing non-degraded and biodegraded examples of GRA and GRB oil types (defined by Lillis et al., 2003). GRA oils (the most common subtype) have a higher wax content, low carbon preferential index (CPI less than 1.10), and low β-carotane content, whereas GRB oils generally have higher odd-carbon predominance (CPI greater than 1.2) and higher β-carotane content. Numbered peaks are the normal alkane carbon number. Pr is pristane, Ph is phytane, and C is β-carotane. Biodegradation scale is zero to ten (Peters et al., 2005); at level 4 normal alkanes are destroyed but acyclic isoprenoids (Pr and Ph) are intact; at level 6 acyclic isoprenoids are destroyed and steranes are slightly depleted and 25-norhopanes formed (mass chromatograms not shown); see Table 1.

sampled (Table 2). The Os data from these units are used for correlation from oil to source rock. Sample preparation follows that outlined by Cumming et al. (2012); all samples are cut, polished, dried and then crushed to a fine powder using no metal contact.

The source rocks used for the hydrous pyrolysis experiments are the Mahogany zone (930923-8; 39°53′12″N, 110°44′58″W; Fig. 1 – MZ) and black shale facies (part of the Douglas Creek Member) (930922-1; 39°50′09″N, 110°47′05″W; Fig. 1 – BSF), details and locations of which are outlined in Ruble et al. (2001). These samples were selected as they have been previously characterised using hydrous pyrolysis experiments. The black shale facies represents the dominant source rock for the Green River petroleum, whereas the Mahogany zone is the most organic-rich unit within the Green River Formation with only minor generation (Ruble et al., 2001; Lillis et al., 2003).

3.2. Re–Os analysis

Re–Os isotopic analyses were carried out at Durham University's TOTAL Laboratory for Source Rock Geochronology and Geochemistry in the Durham Geochemistry Centre using protocols outlined by Selby and Creaser (2003) and Selby et al. (2007). A known weight (100–200 mg) of oil (asphaltene fraction), tar sand extract or gilsonite was digested in a Carius tube with a known amount of ^{190}Os and ^{185}Re tracer solution (spike) and inverse *aqua-regia* (3 ml ~11 N HCl and 8 ml ~15.5 N HNO_3) at 220 °C for 48 h. Inverse *aqua-regia* allows complete sample digestion of the petroleum and ensures sample-spike equilibration. For source rock analyses, 200–500 mg of sample material was digested in 8 ml of Cr^{VI}–H_2SO_4 solution (made from 0.25 g of CrO_3 per 1 ml of 4 N H_2SO_4), replacing the inverse *aqua-regia* as the digesting medium as the Cr^{VI}–H_2SO_4 solution preferentially liberates Re and Os from the organic matter in the source rocks (Selby and Creaser, 2003; Kendall et al., 2004; Rooney et al., 2011). The Re and Os were purified from the inverse *aqua-regia* and Cr^{VI}–H_2SO_4 solutions using Re anion exchange chromatography (HCl–HNO_3) and Os solvent extraction ($CHCl_3$) then micro-distillation, respectively. The purified Re and Os were loaded onto Ni and Pt filaments, respectively, and analysed for their isotopic

Table 2
Re–Os isotope data for the three Green River Formation source rock units.

Sample	Depth (m)	Re (ng/g)	±	Os (pg/g)	±	$^{187}Re/^{188}Os$	±	$^{187}Os/^{188}Os$	±	rho[a]	Os_g[b]	TOC (wt.%)
Douglas Creek Member, Marsing 16 core (39°57′1.4904″N, 111°1′37.527″W)												
M16-43	290.3	9.6	0.0	278.6	2.0	199.2	1.8	1.614	0.019	0.679	1.53	–
M16-37	304.2	23.0	0.1	223.4	1.3	619.6	3.9	2.054	0.014	0.714	1.80	–
M16-27*	323.8	22.6	0.1	341.3	2.3	390.2	3.3	1.831	0.018	0.722	1.67	5.96
M16-26*	323.9	23.6	0.1	333.5	2.6	418.3	4.1	1.861	0.022	0.718	1.69	6.47
M16-25*	324.0	42.6	0.1	490.0	2.8	518.6	3.3	1.950	0.013	0.680	1.73	9.71
M16-24*	324.0	27.8	0.1	393.8	3.0	417.4	4.0	1.854	0.022	0.704	1.68	7.09
M16-23*	324.5	54.9	0.2	341.6	1.9	997.4	6.5	2.336	0.014	0.819	1.92	8.20
M16-22*	324.6	56.0	0.2	343.1	2.1	1015.2	7.1	2.352	0.016	0.790	1.93	–
M16-21*	324.6	62.4	0.2	392.8	2.5	984.8	6.9	2.326	0.017	0.735	1.92	5.42
M16-20*	324.7	40.1	0.1	351.6	1.5	690.2	3.2	2.079	0.008	0.599	1.79	5.53
M16-19*	324.7	24.5	0.1	263.1	1.4	556.4	3.4	1.982	0.013	0.665	1.75	3.53
M16-18*	324.9	29.2	0.1	273.4	1.5	645.0	3.8	2.078	0.013	0.651	1.81	6.39
M16-16*	325.1	21.0	0.1	178.2	1.2	716.3	5.5	2.145	0.019	0.725	1.85	5.71
M16-15*	325.3	22.9	0.1	297.1	1.6	458.1	2.7	1.923	0.012	0.648	1.73	5.23
M16-14*	325.4	16.8	0.1	300.2	1.8	328.6	2.2	1.819	0.014	0.654	1.68	4.87
M16-06	334.2	13.9	0.0	234.9	1.5	348.0	2.7	1.848	0.017	0.694	1.70	–
M16-01	343.3	8.9	0.0	193.7	1.5	268.4	2.6	1.753	0.021	0.704	1.64	–
Douglas Creek Member, Coyote Wash 1 core (40°1′22.224″N, 109°18′38.4834″W)												
CW1-36	1021.7	14.4	0.4	186.1	1.5	453.0	13.6	1.798	0.023	0.266	1.61	–
CW1-40*	1026.0	23.4	0.1	307.8	1.7	445.0	2.9	1.774	0.012	0.682	1.59	6.01
CW1-41*	1026.1	14.6	0.1	258.5	1.9	326.9	3.2	1.654	0.020	0.699	1.52	7.55
CW1-42*	1026.2	10.5	0.0	184.0	1.5	330.0	3.6	1.657	0.022	0.732	1.52	6.83
CW1-44*	1026.5	14.2	0.1	245.4	1.8	331.7	3.3	1.573	0.020	0.702	1.43	7.07
CW1-45*	1026.6	30.3	0.1	256.7	1.5	711.0	4.7	2.028	0.014	0.728	1.73	9.98
CW1-46*	1026.8	34.9	0.1	303.2	1.6	692.4	4.2	2.036	0.013	0.695	1.75	7.44
CW1-48*	1027.0	15.3	0.1	145.4	1.3	627.6	7.4	1.921	0.027	0.756	1.66	2.67
CW1-49*	1027.2	83.5	0.3	298.9	1.8	1830.5	11.1	2.889	0.018	0.712	2.13	7.85
CW1-50*	1027.4	46.6	0.2	412.1	3.8	675.1	7.6	1.963	0.032	0.635	1.68	15.46
CW1-51*	1027.5	11.5	0.0	114.3	1.1	600.3	8.2	1.936	0.030	0.807	1.69	4.97
CW1-53*	1027.7	17.7	0.1	180.5	1.4	584.4	5.9	1.960	0.023	0.751	1.72	–
CW1-54*	1027.8	39.1	0.1	346.0	1.9	674.9	4.1	1.956	0.013	0.645	1.67	24.70
CW1-55*	1028.0	33.8	0.1	385.3	2.1	519.5	3.1	1.879	0.012	0.635	1.66	16.92
CW1-62	1042.9	40.6	1.1	469.8	2.1	502.6	14.3	1.716	0.008	0.108	1.51	–
CW1-69	1045.8	1.1	0.0	65.1	0.6	98.6	3.3	1.606	0.025	0.339	1.57	–
Mahogany zone, Coyote Wash 1 core (40°1′22.224″N, 109°18′38.4834″W)												
CW1-01	672.4	20.2	0.1	346.7	2.0	340.6	2.3	1.766	0.014	0.678	1.62	–
CW1-05*	682.5	15.2	0.1	294.0	2.3	301.1	3.2	1.716	0.022	0.719	1.59	11.28
CW1-06*	682.7	28.0	0.1	486.0	2.9	336.0	2.4	1.746	0.014	0.673	1.61	22.78
CW1-07*	682.8	25.5	0.1	464.1	2.8	320.2	2.3	1.730	0.014	0.673	1.60	22.59
CW1-09*	683.2	26.7	0.1	362.6	4.5	433.0	7.8	1.822	0.048	0.668	1.64	25.82
CW1-10*	683.4	20.8	0.1	383.2	3.0	316.4	3.2	1.735	0.022	0.698	1.60	14.47
CW1-12*	683.6	15.5	0.1	264.2	2.8	344.1	5.3	1.765	0.036	0.721	1.62	9.69
CW1-13*	683.7	15.6	0.1	295.3	2.4	307.1	3.4	1.737	0.023	0.717	1.61	9.39
CW1-14*	683.9	16.7	0.1	326.8	3.3	297.9	4.5	1.717	0.034	0.710	1.59	–
CW1-15*	684.3	11.8	0.0	198.4	2.2	349.0	5.8	1.768	0.037	0.742	1.62	10.30
CW1-16*	684.5	14.6	0.1	286.2	2.3	296.6	3.3	1.730	0.024	0.717	1.61	11.35
CW1-20*	684.9	32.7	0.1	426.9	5.3	451.2	8.5	1.837	0.048	0.684	1.65	28.15
CW1-22*	685.2	39.2	0.1	559.9	4.4	411.3	3.8	1.816	0.023	0.612	1.64	21.14
CW1-23*	685.4	20.1	0.1	366.4	3.2	320.1	3.7	1.737	0.026	0.704	1.60	–
CW1-27	696.8	11.2	0.0	214.0	1.6	304.4	3.1	1.713	0.021	0.716	1.59	–
CW1-31	706.8	33.1	0.1	331.7	1.8	593.2	3.6	1.913	0.013	0.688	1.67	–

All uncertainties are stated as 2σ.
[a] Rho is the associated error correlation at 2σ (Ludwig, 1980).
[b] $Os_g = {}^{187}Os/{}^{188}Os$ isotope ratio calculated at the time of oil generation (25 Ma).
* Sample data taken from Cumming et al. (2012).

compositions and abundances using ID-NTIMS (Creaser et al., 1991; Völkening et al., 1991; Walczyk et al., 1991; Selby and Creaser, 2003).

Uncertainties for $^{187}Re/^{188}Os$ and $^{187}Os/^{188}Os$ ratios and elemental abundances were determined by full-error propagation of uncertainties in Re and Os mass spectrometer

measurements, blank abundances and isotopic compositions, spike calibrations and reproducibility of standard Re and Os isotopic values. Total procedural blanks during this study were 2.9 ± 0.06 pg Re and 0.11 ± 0.02 pg Os (1 SD, $n = 4$, *aqua-regia*), and 14.6 ± 0.16 pg Re and 0.05 ± 0.01 pg Os (1 SD, $n = 3$, Cr^{VI}–H_2SO_4 solution). The blank $^{187}Os/^{188}Os$ isotopic composition for *aqua-regia* are 0.26 ± 0.01 (1 SD, $n = 4$) and 0.61 ± 0.03 (1 SD, $n = 3$) for the Cr^{VI}–H_2SO_4 solution. Throughout the period of this study, the NCIET Re standard produced average $^{185}Re/^{187}Re$ values of 0.598071 ± 0.001510 (1 SD, $n = 67$). The measured difference between the $^{185}Re/^{187}Re$ values and the accepted $^{185}Re/^{187}Re$ value (0.5974; Gramlich et al., 1973) was used to correct for sample mass fractionation. The average $^{187}Os/^{188}Os$ ratio of the Durham Romil Osmium Standard (DROsS) is 0.160892 ± 0.000559 (1 SD, $n = 67$). These Re and Os standard values are indistinguishable from those reported in previous studies (Nowell et al., 2008; Finlay et al., 2012; Rooney et al., 2012). A black shale reference standard, SDO-1 (Devonian-Mississippian Huron Member of the Ohio Shale, a U.S. Geological Survey trace element analysis standard), was also analysed throughout this study in order to determine analytical reproducibility. Four replicate analyses of SDO-1 yielded an average $^{187}Re/^{188}Os$ of 1179.2 ± 12.4 (1 SD) and $^{187}Os/^{188}Os$ of 7.936 ± 0.074 (1 SD). The average Re and Os abundance for SDO-1 is 76.3 ppb $\pm$ 1.21 (1 SD) and 641.2 ppt $\pm$ 7.30 (1 SD). The average Os_i (calculated at 366 Ma) is 0.72 ± 0.04 (1 SD). These values are identical within uncertainty to the values for SDO-1 reported in Du Vivier et al. (2014).

The $^{187}Re/^{188}Os$ and $^{187}Os/^{188}Os$ values, their 2σ uncertainty and the associated error correlation (rho) were regressed using Isoplot (V. 4.15; Ludwig, 1980, 2008) and the ^{187}Re decay constant ($\lambda^{187}Re = 1.666 \times 10^{-11}$ a^{-1}; Smoliar et al., 1996). Source rock and oil $^{187}Os/^{188}Os$ compositions at the time of oil generation (Os_g) were calculated using the age of 25 Ma for oil generation (Ruble et al., 2001) and $\lambda^{187}Re$ (Smoliar et al., 1996).

3.3. Hydrous pyrolysis methodology

Gravel-sized (0.5–2.0 cm) rock fragments of samples from an 18-cm thick bed of the Mahogany zone (~200 g; 930923-8) and a 4-cm thick bed of the black shale facies (~450 g; 930922-1) were matured at peak-bitumen and peak-petroleum generation by isothermal hydrous pyrolysis (Lewan, 1985; Ruble et al., 2001). Peak generation refers to the temperature and time conditions that produce the largest yield of bitumen or oil. The hydrous pyrolysis experiments were conducted in Hastelloy C-276 reactors with carburised surfaces. The Mahogany zone and black shale facies rock fragments were immersed in 400 and 350 ml distilled water, respectively, which is sufficient to maintain a liquid–water phase in contact with the rock fragments at the experimental temperatures. The reactors were sealed and filled with ~6.9 MPa of He and leak-checked using a thermal conductivity leak detector. Temperatures were monitored with Type J thermocouples, which are calibrated against national standards, and remain within ±0.5 °C of the desired temperature. Four hydrous pyrolysis experiments were carried out at 330 °C and 360 °C for 72 h for each sample. These temperatures were selected as they represent peak-bitumen generation and peak-oil generation of the Green River source rock samples (Ruble et al., 2001). These temperatures also provide the best conditions to gain sufficient quantities of oil and bitumen for precise Re and Os isotopic analysis, requiring ~200 mg of oil or bitumen.

Once the experiments had cooled to room temperature, pressure and temperature values were recorded and a sample of head-space gas was collected in an evacuated 30 cm^3 stainless-steel cylinder. Any expelled oil generated in the experiments was collected in three steps: (1) the expelled oil was collected from the surface of the water in the reactor with a Pasteur pipette; (2) the water and minor remaining expelled oil were decanted into a glass separatory funnel allowing the separated oil to concentrate at the funnel stopcock, where it was collected with the same Pasteur pipette; (3) the thin film of expelled oil on the reactor walls, separatory funnel, and Pasteur pipette were rinsed with benzene at room temperature, which was then filtered through a 0.45 μm PTFE filter and concentrated by evaporation of the benzene under a fume hood. The expelled oil collected with a Pasteur pipette as described above, is called 'free oil', whereas expelled oil rinsed from the equipment with benzene is called 'equipment rinse'. The equipment rinse only represents the C_{15+} fraction of the free oil because the benzene evaporation loses the lighter fractions of the oil. The free oil represents the full C_{5+} range. The decanted water was filtered through a 0.45 μm cellulose-acetate/nitrate filter. Rock fragments were removed from the reactor and dried at room temperature (~20 °C) in a HEPA fume hood until their weight was constant within 0.1 g after 4 or more hours. These pyrolysed rock fragments are called 'recovered rock'. For clarity the term 'original rock' refers to the rock sample that has not experienced hydrous pyrolysis.

The soluble organic matter within organic-rich rocks (termed bitumen for the duration of this study) was extracted from both the original rock and recovered rock samples (~100 g) using a Soxhlet apparatus for 24 h with $CHCl_3$. The refluxed solvent was filtered through a 0.45 μm polytetrafluoroethylene (PTFE) filter and the bitumen was concentrated by rotary vacuum evaporation. The bitumen only represents the C_{15+} fraction because evaporation removes lighter fractions. This does not pose a problem for Re–Os analysis as Re and Os are held in the heavier fractions of petroleum (>90% in the asphaltene fraction; Selby et al., 2007). The extracted original and recovered rock was allowed to dry at room temperature (~20 °C) in a HEPA fume hood until their weight was constant (<1% change). These are termed 'extracted rock' for Re–Os analysis. For asphaltene separation from the free oil, the method outlined in Section 3.1.1 was used.

In this study Re–Os analyses following the method outlined in Section 3.2 were conducted on the original rock, recovered rock, extracted rock, bitumen, free oil, equipment rinse and asphaltenes (extracted from the free oil where possible). Re–Os analysis using the Cr^{VI}–H_2SO_4 digestion

method was conducted on an aliquot (~200 to 500 mg) of the powdered rock fragments (~50 g) of the original rock, recovered rock, and extracted rock samples. The rock fragments were powdered using no metal contact. A 200 mg aliquot of the bitumen, free oil, equipment rinse, and asphaltenes were digested using inverse *aqua-regia* for Re–Os analysis.

4. RESULTS

4.1. Re–Os abundances and isotopic ratios of the Green River petroleum

The asphaltene fractions of the oils contain 0.35–15.83 ng/g Re and 18.19–196.72 pg/g Os (Table 3), which is low in comparison to some oil asphaltenes that can reach up to 264 ng/g Re and 1443 pg/g Os (Selby et al., 2007). Using asphaltene percentage abundance established through this study (Table 1), the Green River oil Re and Os abundances can be calculated on a whole-oil basis giving approximately 0.03–2.93 ng/g Re and 0.87–36.39 pg/g Os. Re–Os isotopic data are presented in Table 3 with interpreted geochronology presented in Table 4. The oil samples (not including the tar sands oils or gilsonite) have $^{187}Re/^{188}Os$ ratios ranging from 70.3 to 472.6 and $^{187}Os/^{188}Os$ ratios from 1.466 to 1.863, with one outlier (2.141, sample GRB-824A). When all the oil samples are regressed they yield a Model 3 (assumes that the scatter about the isochron is due to a combination of the assigned uncertainties, plus an unknown but normally distributed variation in the $^{187}Os/^{188}Os$ values) age of 45 ± 31 Ma ($n = 14$, Mean Squared Weighted Deviation [MSWD] = 2.2; Table 4 – Isochron 1). This age does not include outlier sample GRB-824A, which is suggested to be derived from a different source facies than the other samples (see Section 5). The certainty in the oil geochronology is hampered by the low precision in the $^{187}Os/^{188}Os$ ratios because of the very low Os abundances, the associated blank correction, and propagation of all uncertainties.

The oils extracted from the tar sands contain 1.50–65.15 ng/g Re and 87.28–342.24 pg/g Os (Table 3). The tar sands are more enriched than the Green River oils, most probably because the tar sands are more enriched in asphaltene where Re and Os are known to be held (Selby et al., 2007). The tar sands have $^{187}Re/^{188}Os$ ratios ranging from 69.4 to 674.1 and $^{187}Os/^{188}Os$ ratios from 1.447 to 1.939. Geochronology of all of the tar sands yields a Model 3 age of 4 ± 28 Ma ($n = 12$, MSWD = 29; Table 4 – Isochron 2). This does not include the outlying sample, VC03-10, which is thought to be contaminated by oil from another source (see Section 5).

The gilsonite samples are the most consistently enriched of the Green River petroleum phases in Re and Os, with 9.47–51.33 ng/g and 221.76–849.01 pg/g, respectively. The gilsonite $^{187}Re/^{188}Os$ and $^{187}Os/^{188}Os$ ratios show limited variation in comparison to the oil and tar sand samples, ranging from 247.1 to 403.9 and 1.670 to 1.849, respectively. All of the gilsonite samples yield a Model 3 age of 45 ± 42 Ma ($n = 12$, MSWD = 42; Table 4 – Isochron 3). The large uncertainty is attributed to the limited variation in $^{187}Re/^{188}Os$ and $^{187}Os/^{188}Os$ ratios.

4.2. Hydrous pyrolysis results

The total recovery for each of the individual hydrous pyrolysis experiments is over 98%, indicating reliable closed-system pyrolysis (see Table 5). All the experiments generated bitumen, oil and gas, with the largest amount of oil generated during the 360 °C (peak-oil) experiments, and the largest amount of bitumen generated at the 330 °C (peak-bitumen) experiments (Table 6). These results support the findings of Ruble et al. (2001) and provide sufficient organic material for Re–Os analysis.

4.2.1. Re and Os abundances of hydrous pyrolysis products

Rhenium and Os abundance data from the hydrous pyrolysis experiments are reported as ng/g of original rock using the equation:

$$\{M_i\} = [(A_i * g_i)/1000]/G$$

where the subscript '*i*' refers to the material (original rock, recovered rock, extracted rock, bitumen, etc.) being analysed, A is abundance in ng/g, g is weight of material in grams, and G is weight of starting rock in grams (Rooney et al., 2012). Presenting the data in this format allows mass balance calculations to evaluate Re and Os abundances located in the various fractions and to more accurately interpret the transfer behaviour and mechanisms of Re and Os in the source rock and petroleum system relative to each other. The abundance data are presented in Table 7 for all the experiments. The Re–Os isotopic compositions are reported in Table 8.

In both the Mahogany zone and black shale facies, the Re and Os contents of original rock, recovered rock, and extracted rock are similar (Table 7). Analyses of these sets of rock samples are conducted on an aliquot of powdered rock fragments (~50 g) that are randomly selected from a bag containing ~200–400 g of ~1 cm-sized rock chips. Over 20 g is powdered in order to obtain a homogenised representation of the Re–Os abundance and isotope composition of the rock sample (Kendall et al., 2009). The small variations in Re and Os abundances are attributed to minor differences of the randomly selected rock fragments used for each Re–Os analysis. The Re and Os abundances of the Mahogany zone and black shale facies original rocks are 24.6 and 0.337 ng/g original rock, and 3.88 and 0.161 ng/g original rock, respectively. For all the rock sample aliquots analysed after the hydrous pyrolysis experiments the Re and Os abundances are within 10–15% of the original rock value (Table 7).

The bitumen that was extracted from the original rocks contained low Re and Os abundances of 0.284 and 0.003 ng/g original rock (Mahogany zone), and 0.010 and 0.001 ng/g original rock (black shale facies), respectively. The 330 °C experiment represents the peak-bitumen generation (as demonstrated by Ruble et al., 2001). Extracted bitumen from the recovered Mahogany zone rock (330 °C experiment) contains 0.231 ng/g original rock Re and 0.018 ng/g original rock Os. In comparison, the extracted bitumen from the black shale facies 330 °C experiment contains less Re (0.138 ng/g original rock Re), and very small amounts of Os (0.008 ng/g original rock).

Table 3
Re–Os isotope data for the Green River petroleum system hydrocarbons.

Sample	Re (ng/g)	±	Os (pg/g)	±	$^{187}Re/^{188}Os$	±	$^{187}Os/^{188}Os$	±	rho[a]	Os_i[b]	Os_i[c]
Re–Os data for the Green River oils											
GR2242A	0.61	0.03	49.51	1.77	70.3	6.2	1.466	0.164	0.555	1.44	1.44
GR2264A	0.97	0.03	26.04	0.93	211.4	18.9	1.527	0.142	0.818	1.44	1.46
GR2269A	0.78	0.03	30.97	0.94	144.8	11.0	1.588	0.125	0.746	1.44	1.54
GR2232A	0.35	0.03	18.63	0.76	106.9	13.5	1.485	0.157	0.697	1.44	1.45
GR2266A	0.38	0.03	18.20	0.84	119.8	16.7	1.504	0.180	0.734	1.45	1.47
GR2267A	1.20	0.03	45.14	1.21	152.7	9.6	1.565	0.110	0.738	1.50	1.52
GR2239A	2.09	0.03	73.87	1.72	163.4	7.9	1.630	0.100	0.721	1.56	1.58
GRB-3885A	1.33	0.03	47.61	1.22	160.7	9.2	1.643	0.110	0.735	1.58	1.59
GRB-1602A	3.05	0.03	144.82	3.16	121.2	5.1	1.629	0.094	0.702	1.58	1.59
GR2268A	0.86	0.04	18.19	0.96	275.5	37.8	1.715	0.236	0.893	1.60	1.63
GRB-827A	15.83	0.06	196.72	4.34	472.6	19.5	1.807	0.104	0.711	1.61	1.66
GR2114A	3.36	0.03	62.07	1.51	316.8	15.7	1.774	0.112	0.757	1.64	1.67
GRB-847A	2.33	0.04	80.17	1.99	169.9	9.0	1.748	0.113	0.733	1.68	1.69
GR2259A	1.62	0.04	48.19	1.38	199.0	12.9	1.863	0.139	0.765	1.78	1.80
GRB-824A	1.75	0.07	60.69	2.16	175.4	15.7	2.141	0.198	0.786	2.07	2.09
Re–Os data for the Green River tar sands											
VC03-10	65.15	0.21	95.89	0.95	4021.7	65.8	1.878	0.031	0.940	0.20	0.60
VC25-10	17.75	0.06	151.08	1.36	674.1	9.2	1.590	0.026	0.776	1.31	1.38
VC15-10	5.49	0.16	342.24	4.33	90.6	3.3	1.447	0.042	0.412	1.41	1.42
VC32-10	11.24	0.33	143.11	1.37	452.7	14.6	1.627	0.029	0.359	1.44	1.48
VC02-10	10.16	0.04	116.78	1.43	506.4	10.5	1.724	0.043	0.793	1.51	1.56
VC04-10	9.29	0.04	95.86	1.48	567.0	15.9	1.766	0.061	0.794	1.53	1.59
VC20-10	4.44	0.13	94.02	1.42	272.8	10.9	1.649	0.056	0.533	1.54	1.56
VC14-10	11.92	0.05	183.30	1.83	379.1	5.9	1.733	0.032	0.786	1.57	1.61
VC01-10	5.50	0.04	97.38	1.54	329.1	9.7	1.723	0.061	0.789	1.59	1.62
VC35-10	6.43	0.04	129.95	1.85	287.5	7.1	1.706	0.054	0.740	1.59	1.61
VC33-10	1.50	0.04	124.25	1.84	69.4	2.5	1.622	0.054	0.576	1.59	1.60
VC11-10	4.24	0.13	167.09	2.32	149.4	5.6	1.824	0.055	0.449	1.76	1.78
VC10-10	4.28	0.03	87.28	1.36	292.1	8.2	1.939	0.066	0.772	1.82	1.85
Re–Os data for the Green River gilsonite											
VC12-10	21.48	0.62	359.33	2.71	347.0	10.5	1.693	0.021	0.227	1.55	1.58
VC47-10	24.32	0.09	431.97	2.80	327.0	2.7	1.702	0.016	0.696	1.57	1.60
VC16-10	9.47	0.04	221.76	2.00	247.1	3.3	1.670	0.027	0.730	1.57	1.59
VC05-10	26.84	0.09	399.95	2.83	391.3	3.5	1.737	0.019	0.694	1.57	1.61
VC46-10	28.71	0.10	490.41	3.21	341.4	2.7	1.740	0.017	0.670	1.60	1.63
VC45-10	25.07	0.09	426.70	2.74	342.8	2.7	1.744	0.016	0.686	1.60	1.64
VC44-10	34.46	0.12	499.20	3.18	403.9	3.0	1.769	0.016	0.670	1.60	1.64
VC08-10	22.10	0.08	343.99	2.73	376.0	3.9	1.771	0.023	0.716	1.61	1.65
VC07-10	24.95	0.09	412.87	2.89	353.7	3.1	1.773	0.019	0.696	1.63	1.66
VC06-10	33.29	0.11	500.91	4.28	389.8	4.3	1.793	0.026	0.682	1.63	1.67
VC34-10	33.42	0.96	538.62	3.21	364.1	10.7	1.797	0.014	0.155	1.64	1.68
VC09-10	51.33	0.17	849.01	4.26	356.8	1.9	1.849	0.011	0.598	1.70	1.74

All uncertainties are stated as 2σ.
[a] Rho is the associated error correlation at 2σ (Ludwig, 1980).
[b] $Os_i = {}^{187}Os/{}^{188}Os$ isotope ratio calculated at 25 Ma.
[c] $Os_i = {}^{187}Os/{}^{188}Os$ isotope ratio calculated at 19 Ma.

During both 360 °C experiments, which represent peak-oil generation, most of the bitumen has been converted to oil. For both rock types the extracted bitumen contains only very minor Re and Os (<0.001 ng/g original rock). In both the Mahogany zone and black shale facies experiments, Re and Os concentrations increased by an order of magnitude from the original rock bitumen to the recovered rock bitumen (330 °C experiment), although the Mahogany zone bitumen is an exception and Re does not increase. However, in the bitumen extracted from the recovered rock in the 360 °C experiments Re and Os concentrations decreased by two orders of magnitude from the 330 °C experiment bitumen.

In all the experiments, there is limited transfer of Re and Os to the free oil collected as well as the equipment rinse, which incorporates the rest of the oil produced. Thus the change in Re and Os abundance in the bitumen from the original rock and the 330° and 360 °C experiments cannot be explained by transfer to the generated oil. The asphaltenes extracted from the free oil of the 360 °C experiments have also been analysed because this is the location of >90% of the Re and Os in oil and thus gives higher

Table 4
Re–Os geochronology results.

Isochron No.	Description	n	Ma	±	MSWD	Model	Os_i	±	Samples
1	Oils	14	45	31	2.2	3	1.50	0.12	GR2242A, GR2264A, GR2269A, GR2232A, GR2266A, GR2267A, GR2239A, GRB-3885A, GRB-1602A, GR2268A, GRB-827A, GR2114A, GRB-847A, GR2259A
2	Tar sands	12	4	28	29	3	1.67	0.18	VC25-10, VC15-10, VC32-10, VC02-10, VC04-10, VC20-10, VC14-10, VC01-10, VC35-10, VC33-10, VC11-10, VC10-10
3	Gilsonite	12	45	42	42	3	1.49	0.25	VC05-10, VC06-10, VC07-10, VC08-10, VC09-10, VC12-10, VC34-10, VC16-10, VC44-10, VC45-10, VC46-10, VC47-10
4	All samples	38	19	14	30	3	1.61	0.08	GR2242A, GR2264A, GR2269A, GR2232A, GR2266A, GR2267A, GR2239A, GRB-3885A, GRB-1602A, GR2268A, GRB-827A, GR2114A, GRB-847A, GR2259A, VC25-10, VC15-10, VC32-10, VC02-10, VC04-10, VC20-10, VC14-10, VC01-10, VC35-10, VC33-10, VC11-10, VC10-10, VC05-10, VC06-10, VC07-10, VC08-10, VC09-10, VC12-10, VC34-10, VC16-10, VC44-10, VC45-10, VC46-10, VC47-10
5	All samples without gilsonite	26	15	17	14	3	1.60	0.09	GR2242A, GR2264A, GR2269A, GR2232A, GR2266A, GR2267A, GR2239A, GRB-3885A, GRB-1602A, GR2268A, GRB-827A, GR2114A, GRB-847A, GR2259A, VC25-10, VC15-10, VC32-10, VC02-10, VC04-10, VC20-10, VC14-10, VC01-10, VC35-10, VC33-10, VC11-10, VC10-10
6	$Os_i = 1.40–1.55$	12	33	12	6.6	3	1.45	0.07	GR2242A, GR2264A, GR2269A, GR2232A, GR2266A, GR2267A, VC15-10, VC32-10, VC02-10, VC04-10, VC20-10, VC12-10
7	$Os_i = 1.55–1.70$	21	29.9	9.5	4.7	3	1.57	0.06	GR2239A, GRB-3885A, GRB-1602A, GR2268A, GRB-827A, GR2114A, GRB-847A, GR2259A, VC14-10, VC01-10, VC35-10, VC33-10, VC05-10, VC06-10, VC07-10, VC08-10, VC34-10, VC16-10, VC44-10, VC45-10, VC46-10, VC47-10
8	$Os_i = 1.40–1.55$ without gilsonite	11	32	11	2.9	3	1.44	0.07	GR2242A, GR2264A, GR2269A, GR2232A, GR2266A, GR2267A, VC15-10, VC32-10, VC02-10, VC04-10, VC20-10
9	$Os_i = 1.55–1.70$ without gilsonite	11	22.6	9.6	0.53	1	1.60	0.05	GR2239A, GRB-3885A, GRB-1602A, GR2268A, GRB-827A, GR2114A, GRB-847A, GR2259A, VC14-10, VC01-10, VC35-10, VC33-10
10	Non-biodegraded oils ($Os_i = 1.40–1.55$)	6	29	78	0.44	1	1.47	0.19	GR2242A, GR2264A, GR2269A, GR2232A, GR2266A, GR2267A
11	Non-biodegraded oils ($Os_i = 1.55–1.70$)	5	25	23	0.92	1	1.62	0.12	GR2239A, GR2268A, GRB-827A, GR2114A, GRB-847A
12	Tar sands ($Os_i = 1.55–1.70$)	7	15.6	7.5	1.15	1	1.62	0.05	VC02-10, VC04-10, VC20-10, VC14-10, VC01-10, VC35-10, VC33-10
13	GRA hydrocarbons	22	15	20	16	3	1.60	0.11	GR2242A, GR2264A, GR2269A, GR2232A, GR2266A, GR2267A, GR2239A, GR2268A,GR2114A, GR2259A, VC25-10, VC15-10, VC32-10, VC02-10, VC04-10, VC20-10, VC14-10, VC01-10, VC35-10, VC33-10, VC11-10, VC10-10
14	GRB hydrocarbons	16	31	19	30	3	1.58	0.11	GRB-3885A, GRB-1602A, GRB-827A, GRB-847A, VC05-10, VC06-10, VC07-10, VC08-10, VC09-10, VC12-10, VC34-10, VC16-10, VC44-10, VC45-10, VC46-10, VC47-10

n = number of samples.
The outliers GRB-824A and VC03-10 described in the text are not included in this table.
Os_i is calculated at 25 Ma (see text).
Model number from Ludwig (2008).

Table 5
Hydrous pyrolysis conditions and details of yields.

Sample and temperature (°C)	Rock at start (g)	Water in reactor (g)	Recovered rock (g)	Water recovered (g)	Generated gas (g)	Expelled oil (g)	Total recovery (%)
M 930923-8, 330 °C/72 h	200.3	400.0	185.0	399.1	4.00	4.21	98.67
M 930923-8, 360 °C/72 h	200.0	400.6	168.1	399.5	7.10	18.08	98.70
BS 930922-1, 330 °C/72 h	450.1	350.5	435.7	344.0	4.50	4.02	98.45
BS 930922-1, 360 °C/72 h	450.4	350.2	421.8	348.8	6.90	14.03	98.87

Table 6
Organic phases recovered from the hydrous pyrolysis experiments.

Sample and temperature (°C)	TOC (wt.%)	Bitumen (mg/g orig.TOC)	Expelled oil (mg/g orig.TOC)	Generated gas (mg/g orig.TOC)	Total (mg/g orig.TOC)
M 930923-8	15.23	157.24	–	–	–
M 930923-8, 330 °C/72 h	15.23	576.14	276.43	262.64	1115.20
M 930923-8, 360 °C/72 h	15.23	140.20	1186.93	466.19	1793.32
BS 930922-1	5.86	145.22	–	–	–
BS 930922-1, 330 °C/72 h	5.86	682.95	686.01	767.92	2136.87
BS 930922-1, 360 °C/72 h	5.86	276.43	2394.54	1177.47	3848.45

precision measurements. The asphaltenes contain 5.1 and 1.3 ng/g Re and 0.049 and 0.036 ng/g Os for the Mahogany zone and black shale facies free oils, respectively. This suggests that there must at least be minor transfer of Re and Os to the free oil from the bitumen.

In the Mahogany zone experiments the mass balance calculations show discrepancies within 10%, suggesting only minor loss or addition of Re and Os during the experimental procedure. In the black shale facies experiments there are nearly 20% discrepancies in the mass balance for Re, particularly during the 330 °C experiment. These discrepancies may reflect variation in aliquots used for analysis. Kendall et al. (2009) show that repeat analysis of crushed rock samples of <10 g can yield up to 4% discrepancies in abundances of Re and Os, whereas repeat analysis of powdered samples obtained from >20 g of rock yield reproducibility of <3%. Here ~50 g of randomly selected rock chips from the ~200 and 450 g aliquots used in the hydrous pyrolysis experiments were selected (see Table 5). Thus, it is likely that the variations seen in this study are largely controlled by the variation in aliquots used that have slightly different Re and Os abundances and isotopic compositions, which was also observed for the Re–Os hydrous pyrolysis experiments of the Phosphoria and Staffin Formations (Rooney et al., 2012).

4.2.2. Re–Os isotopic data for the hydrous pyrolysis products

The $^{187}Re/^{188}Os$ and $^{187}Os/^{188}Os$ data are reported in Table 8 and Fig. 3. Several of the bitumen Re–Os data have large uncertainties associated with them related to the small sample size and very low Re and Os abundances and the associated propagation of blank uncertainties (Table 7). The free oil and equipment rinse ratios had uncertainties up to and over 100% of their values due to the negligible contents and consequently isotopic compositions are not reported. The $^{187}Re/^{188}Os$ and $^{187}Os/^{188}Os$ ratios in the original rock and extracted rock, and the recovered rock and extracted recovered rock from each experiment show no variation within uncertainty. The $^{187}Re/^{188}Os$ ratios, however, decrease from 427.4 (original) to 367.3 (330 °C) and then increase again to 420.2 (360 °C) in the Mahogany zone (see Fig. 3). For the black shale facies a similar pattern occurs, decreasing from 138.8 (original) to 120.5 (330 °C) and then increasing to 129.3 (360 °C). The $^{187}Os/^{188}Os$ ratios remain similar throughout, at ~1.8 for the Mahogany zone rocks and ~1.6 for the black shale facies.

The bitumen from the original rock and 330 °C experiments show in all cases that the $^{187}Re/^{188}Os$ values decrease, apart from in the bitumen extracted from the original rock of the Mahogany zone, where the values increase, from 427.4 to 596.0. For $^{187}Os/^{188}Os$ ratios of the bitumen, the values all stay the same at ~1.8 (Mahogany zone) and ~1.6 (black shale facies), again apart from in the original rock of the Mahogany zone, where the values are ~2.0. The Re–Os isotope compositions for bitumen for the 360 °C experiments are not considered because the negligible abundances in these fractions have led to large uncertainties. The asphaltenes derived from the free oil of the peak-oil generation (360 °C) experiments, show an increase in $^{187}Re/^{188}Os$ values from the recovered rock and a minor decrease in the $^{187}Os/^{188}Os$ ratios in the Mahogany zone to 1.5, but staying the same at ~1.6 for the black shale facies. Fig. 3 illustrates that the hydrous pyrolysis experiments have a more significant effect on the Mahogany zone with larger variations in $^{187}Re/^{188}Os$ values than the black shale facies and also some variation in $^{187}Os/^{188}Os$ ratios in the bitumen extracted from the original rock and the asphaltene extracted from the free oil of the peak-oil 360 °C experiment.

5. DISCUSSION

5.1. Dating petroleum generation in the Green River petroleum system

Many petroleum systems, the Green River included, are complex and involve multi-stage/ongoing generation from a number of source rock intervals, with resulting mixtures of

Table 7
Mahogany zone and black shale facies Re and Os contents of original rock, recovered rock, extracted rock, bitumen, free oil and equipment rinse.

Fraction	Mahogany 930923-8								Black Shale Facies 930922-1							
	Re (ng/g fraction)		Re	Re	Os (ng/g fraction)		Os	Os	Re (ng/g fraction)		Re	Re	Os (ng/g fraction)		Os	Os
	Mean	±	(ng/g orig rock)	D%*	Mean	±	(ng/g orig rock)	D%*	Mean	±	(ng/g orig rock)	D%*	Mean	±	(ng/g orig rock)	D%*
Original Rock																
Original Rock	24.61	0.09	24.609		0.337	0.002	0.337		3.88	0.02	3.876		0.161	0.002	0.161	
Extracted Rock	28.31	0.09	27.634		0.389	0.002	0.380		3.90	0.02	3.871		0.162	0.002	0.161	
Bitumen	11.86	0.05	0.284		0.119	0.001	0.003		1.12	0.03	0.010		0.107	0.001	0.001	
Total**			27.918	113.4			0.383	113.6			3.880	100.1			0.162	100.5
330 °C for 72 h																
Recovered Rock	24.30	0.08	22.442		0.387	0.002	0.357		3.17	0.02	3.071		0.152	0.002	0.147	
Free Oil	0.03	0.03	0.000		0.006	0.001	0.000		0.81	0.03	0.007		0.018	0.001	0.000	
Equipment Rinse	0.08	0.03	0.001		0.023	0.001	0.000		ND				ND			
Total***			22.443	91.2			0.357	106.1			3.078	79.4			0.147	91.3
Extracted Rock	26.55	0.09	22.191		0.394	0.002	0.330		3.14	0.02	2.912		0.147	0.002	0.136	
Bitumen	2.64	0.03	0.231		0.200	0.002	0.018		3.44	0.03	0.138		0.198	0.002	0.008	
Total**			22.423	99.9			0.347	97.2			3.050	99.3			0.144	98.1
360 °C for 72 h																
Recovered Rock	28.94	0.10	24.325		0.402	0.002	0.338		3.64	0.02	3.409		0.162	0.002	0.152	
Free Oil	0.05	0.03	0.004		0.002	0.001	0.000		0.11	0.03	0.002		0.003	0.001	0.000	
Equipment Rinse	0.03	0.03	0.000		0.011	0.001	0.000		0.02	0.03	0.000		0.007	0.001	0.000	
Total***			24.329	98.9			0.339	100.5			3.411	88.0			0.152	94.4
Extracted Rock	28.55	0.09	23.390		0.401	0.002	0.328		4.01	0.02	3.689		0.167	0.002	0.153	
Bitumen	0.03	0.03	0.001		0.003	0.001	0.000		0.03	0.03	0.000		0.009	0.001	0.000	
Total**			23.390	96.2			0.328	97.1			3.690	108.2			0.153	101.0

ND = Not Determined.
* Re D% and Os D% = Total metal (extracted rock + bitumen)/Recovered rock × 100 or Total metal (recov. rock + oil + equip. rinse)/original rock × 100.
** Total = Extracted rock + Bitumen.
*** Total = Recovered rock + Free Oil + Equipment Rinse.

Table 8
Mahogany zone and black shale facies Re–Os isotopic compositions of original rock, recovered rock, extracted rock, bitumen, and asphaltene* fraction of the free oil.

Fraction	Mahogany 930923-8				Black Shale Facies 930922-1			
	$^{187}Re/^{188}Os$		$^{187}Os/^{188}Os$		$^{187}Re/^{188}Os$		$^{187}Os/^{188}Os$	
	Mean	±	Mean	±	Mean	±	Mean	±
Original Rock	427.4	3.1	1.768	0.014	138.8	2.3	1.640	0.033
Extracted Rock	425.5	2.6	1.766	0.012	138.7	2.2	1.641	0.033
Bitumen	596.0	10.9	2.008	0.040	59.9	2.0	1.607	0.034
330 °C for 72 h								
Recovered Rock	367.3	2.1	1.761	0.011	120.5	2.1	1.631	0.033
Extracted Rock	393.7	2.4	1.761	0.012	123.3	2.1	1.630	0.034
Bitumen	77.2	1.3	1.765	0.026	99.8	1.5	1.615	0.024
360 °C for 72 h								
Recovered Rock	420.2	2.4	1.756	0.011	129.3	2.1	1.626	0.033
Extracted Rock	416.3	2.5	1.754	0.011	138.4	2.2	1.613	0.033
Bitumen	46.6	59.8	0.949	0.536	16.6	17.9	0.320	0.070
Asphaltene*	590.3	23.7	1.519	0.062	209.9	13.7	1.590	0.096

* Asphaltenes contain 5.1 and 1.3 ng/g Re and 48.9 and 35.9 pg/g Os for the Mahogany zone and black shale facies free oils, respectively.

oil of different ages or from different sources. If this is the case, care must be taken when interpreting Re–Os data for geochronology. In the Phosphoria petroleum system a complex and lengthy generation and migration history coupled with a large source rock interval are interpreted to cause scatter about the Re–Os isochron (Lillis and Selby, 2013). However, oils from the UK Atlantic margin provide Re–Os geochronology, although imprecise (±20%), in excellent agreement with oil generation models and Ar–Ar ages of feldspars containing oil inclusions (Finlay et al., 2011). In addition, Re–Os geochronology studies of the Western Canadian oil sands (Selby and Creaser, 2005a) and bitumen associated with the Polaris Mississippi Valley-type Zn–Pb deposit (Selby et al., 2005), have provided Re–Os geochronology in agreement with generation models, the latter also agreeing with an Rb–Sr sphalerite date of co-genetic mineralisation. Based on these previous studies and the assumption that Re and the $^{187}Os/^{188}Os$ ratio of the source rock is transferred to the produced petroleum at the time of generation and that there is no post-generation addition or removal of Re and Os, we consider the Re–Os ages for petroleum to reflect a generation age.

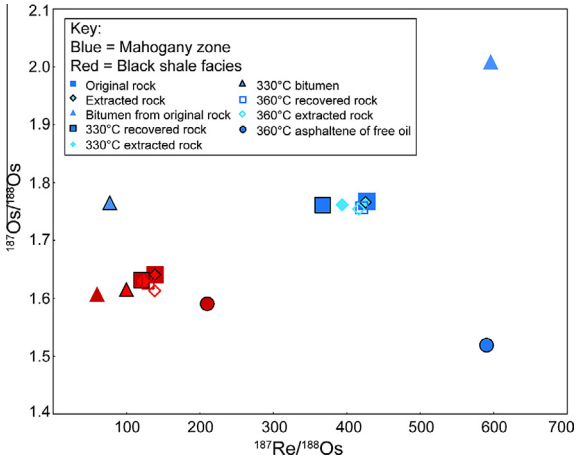

Fig. 3. Re–Os isotopic data for the products derived from the hydrous pyrolysis experiments for both source units used. The Mahogany zone (930923-8) is shown in blue and the black shale facies (930922-1) in red. Bitumen from the 360 °C experiment is not shown due to the large uncertainties derived from very low abundances of Re and Os in this bitumen. (For interpretation of the references to colour in this figure legend, the reader is referred to the web version of this article.)

5.1.1. Previous generation models

The Uinta Basin is currently an active petroleum system (Fouch et al., 1994; Ruble et al., 2001). Early oil generation models based on Rock–Eval pyrolysis kinetic parameters show oil generation beginning as early as 40 Ma in the lower part of the Green River Formation, with the majority of generation in the Douglas Creek Member (containing the black shale facies) between 30 and 20 Ma, and with generation moving up-section to the Mahogany zone from 20 Ma to the present day (Sweeney et al., 1987; Anders et al., 1992; Fouch et al., 1994). More recent hydrous pyrolysis kinetic models suggest that oil generation began in the lower part of the Green River Formation around 25 Ma, with generation moving upsection with time through the Douglas Creek Member, but significant generation from the Mahogany zone is unlikely (middle part of the Parachute Creek Member; Ruble et al., 2001). It is suggested that hydrous pyrolysis kinetic parameters for immiscible oil generation are generally consistent with observed oil generation data from natural petroleum systems (Ruble et al., 2001; Lewan and Ruble, 2002; Lewan and Roy, 2011). As the Green River petroleum system has ongoing petroleum generation (most reservoirs are overpressured), the reservoirs likely contain a mixture of oils from the Green River Formation source rocks.

5.1.2. Re–Os petroleum generation geochronology

Geochronology of all the samples yields a Model 3 age of 19 ± 14 Ma ($n = 38$, MSWD = 30; Table 4, Isochron 4; Fig. 4A). Despite the large uncertainty, this age broadly agrees with previous oil generation models, but most closely

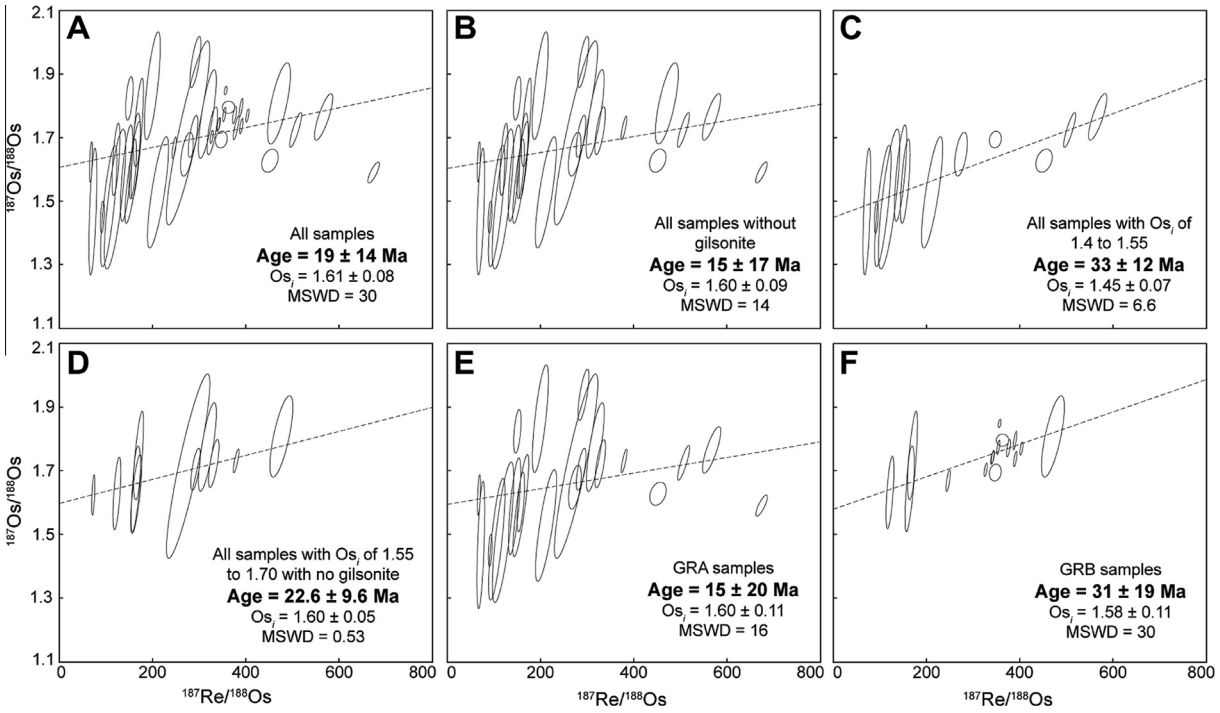

Fig. 4. Re–Os isochrons for the Green River petroleum, showing the age data derived. Uncertainty ellipses are 2σ. See Table 4 and text for further details. A = Isochron 4, B = Isochron 5, C = Isochron 6, D = Isochron 9, E = Isochron 13, F = Isochron 14 (Table 4).

agrees with generation beginning at 25 Ma (Ruble et al., 2001). Two samples (GRB-824A and VC03-10) have been excluded from all Re–Os geochronology calculations as they potentially represent contamination or a different source. The GRB-824A oil sample is derived from the Red Wash field (Table 1), where oil is thought to be derived from Paleocene to lower Eocene source rocks dissimilar to the other Green River Formation source rocks (Picard, 1957; Anders et al., 1992). The VC03-10 tar sand sample has a drastically different $^{187}Re/^{188}Os$ ratio (4021.7) from the other samples and also a different Os_i of 0.20, which we suggest is due to contamination from another oil source in the region as these ratios cannot have been inherited from the Green River Formation. When each of the oils, tar sands and gilsonite are regressed separately, they yield imprecise Model 3 ages with large MSWD's (Isochrons 1 to 3 – Table 4). A Model 3 age, large uncertainty, and an MSWD much higher than 1 suggest scatter about the linear regression is related to geological factors rather than purely analytical uncertainties (Ludwig, 2008). We suggest that this is due to the variation in Os_i of the oils and tar sand samples which could easily cause scatter as the isochron technique fundamentally requires samples to have the same Os_i, but variable $^{187}Re/^{188}Os$ values (Cohen et al., 1999). It also requires samples to have been formed at the same time or generated at the same time and not to have undergone post-formational geochemical alteration (Lillis and Selby, 2013). Thus, the large uncertainty in the oil and tar sand ages may be caused by variation in the Os_i (1.44–1.78 and 1.31–1.82 at 25 Ma, for oils and tar sands respectively; Table 3) derived from a mixture of oils from different sources (within the Green River Formation) and generated at different times. The variation in Os_i (1.58–1.74 at 25 Ma; Table 3) for the gilsonite is much lower than the tar sands or oils, but the age is imprecise (93% uncertainty). If formation of gilsonite occurs by sudden expulsion (Verbeek and Grout, 1992), then one would expect homogenous Os isotope compositions derived from the same source at the same time. Considering that the mechanism and timing of emplacement is poorly constrained and the unusual nature of the gilsonite deposits, it is uncertain what may be the main control on the Re–Os system in gilsonite, however the large uncertainty could also be caused by the limited spread in $^{187}Re/^{188}Os$ ratios (~150 units). The limited spread in $^{187}Re/^{188}Os$ and $^{187}Os/^{188}Os$ ratios would support the idea of rapid expulsion for the gilsonite deposits as well as a single source unit producing the deposits. The tar sands are migrated deposits of the Green River oils (Fouch et al., 1994) and so they can be grouped together with the oils for Re–Os geochronology. Regression of all the samples without the gilsonite gives an age of 15 ± 17 Ma ($n = 26$, MSWD = 14; Table 4 – Isochron 5; Fig. 4B), however, the large range in Os_i still affects the precision of this age.

5.1.2.1. Re–Os geochronology based on Os_i composition. The variation in Os_i composition for all the petroleum samples can be plotted on a histogram showing the most common values (Fig. 5). When the Os_i values are calculated at 25 Ma to reflect the oil generation models, distinct Os_i data clusters are evident. The histogram (Fig. 5) shows that the mode is at 1.6 and there are two smaller data clusters at 1.4 and 1.5. Calculation of the Os_i at 19 Ma reflecting the Re–Os age of all the petroleum samples yields similar clusters of the Os_i data; a mode at 1.6 and other clusters at 1.5

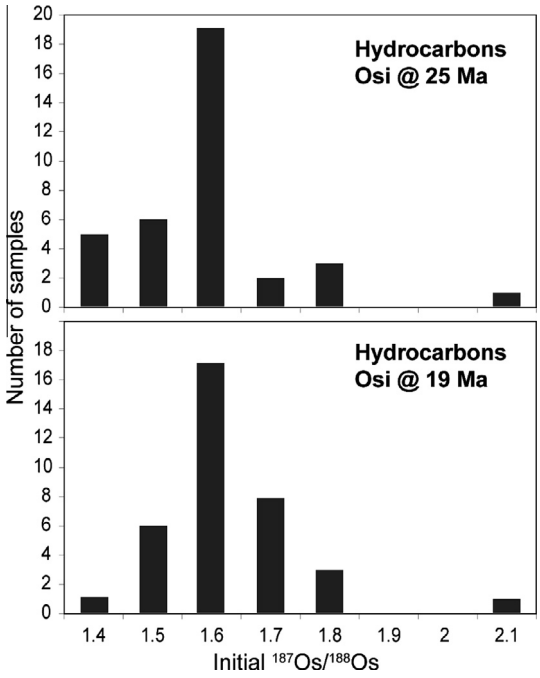

Fig. 5. Histograms giving a visual impression of the distribution of Os_i data. Histograms for the petroleum show Os_i calculated at 25 Ma and 19 Ma. Os_i calculation is based on the Re–Os isotopic data, the λ^{187}Re of Smoliar et al. (1996) and age of petroleum generation.

and 1.7. Fig. 5 demonstrates that the calculation at a younger age yields slightly more radiogenic Os_i, but does not alter the relationship of the samples to each other and so the age used for calculation of Os_i does not skew the oil mode and hence does not adversely affect geochronology based on Os_i composition. The different Os_i values are interpreted to reflect variation in Os composition of the Green River Formation source rock that is then transferred to the generated petroleum phases. Regressing the Re–Os data based on Os_i would reflect geochronology of oils derived from different Green River Formation source units (see Section 5.2.2). Based on the Os_i calculated at 25 Ma, the mode of the samples is 1.6; these can be grouped with the few samples at 1.7, giving a group with Os_i between 1.55 and 1.70. A second smaller group with Os_i from 1.4 to 1.55 represents the largest number of samples outside the mode. All samples with Os_i from 1.40 to 1.55 yield an age of 33 ± 12 Ma ($n = 12$, MSWD = 6.6, Model 3; Table 4 – Isochron 6; Fig. 4C) and samples with Os_i from 1.55 to 1.70 yield an age of 29.9 ± 9.5 Ma ($n = 21$, MSWD = 4.7, Model 3; Table 4 – Isochron 7). Separating the samples based on Os_i provides higher precision dates with lower MSWD's compared to the isochrons including samples with variable Os_i. Justification for this method comes from the fundamental aspect of Re–Os geochronology that requires samples to possess a common Os_i value to produce a precise isochron (York, 1969; Cohen et al., 1999; Kendall et al., 2009). Additionally, the multimodal Os_i suggests discrete source units produced the petroleum (Selby et al., 2007; Finlay et al., 2011, 2012; Rooney et al., 2012; Lillis and Selby, 2013). This approach can also be used for isochrons of all the petroleum samples excluding the gilsonite (Isochrons 8 and 9 – Table 4), as the gilsonite may have been generated by a different process at a different time (Tetting, 1984; Verbeek and Grout, 1992). This only significantly affects the 1.55–1.70 group as most of the gilsonite lies within this range. The Re–Os data give a Model 1 (assumes that the assigned uncertainties are the only reason for the scatter in the linear regression) age of 22.6 ± 9.6 Ma ($n = 11$, MSWD = 0.53; Table 4 – Isochron 9; Fig. 4D) for the oils and tar sands. All the ages produced agree within uncertainty, but this Model 1 age suggests any scatter is related to uncertainties in the analytical procedure rather than geological uncertainties. This age is consistent with the modelled age of the beginning of oil generation in the lower part of the Green River Formation around 25 Ma (Ruble et al., 2001) and suggests that the Re–Os geochronometer of petroleum records the timing of oil generation.

5.1.2.2. Effects of biodegradation. The Os_i groupings can also be plotted for each of the oils and tar sands separately as this shows a distinction between biodegraded (tar sands; Isochron 12 – Table 4) and non-biodegraded (oils; Isochrons 10 and 11, Table 4) samples. Two oil samples, GRB-3885 and GRB-1602, show slight biodegradation (Table 1) and as a result are removed from the non-biodegraded oil isochrons. Isochrons 10, 11, and 12 (Table 4) give Model 1 ages, with low MSWD's that are within uncertainty of each other. The lack of precision on the oil isochrons is related to the uncertainty on the $^{187}Os/^{188}Os$ measurements that are challenging due to the low Os abundances, blank correction, and propagation of all sources of uncertainty (Table 3). The age for the heavily biodegraded tar sands (Isochron 12) is similar to the Ruble et al. (2001) generation models (oil generation began in the lower part of the Green River Formation at 25 Ma) and is within uncertainty of the other ages produced, which suggests that biodegradation has not adversely affected the Re–Os systematics of Type I lacustrine kerogen derived petroleum. This agrees with previous Re–Os studies that have proposed that the Re–Os isotope system is not adversely affected by biodegradation (Selby et al., 2005; Selby and Creaser, 2005a; Finlay et al., 2011, 2012).

5.1.2.3. Influence of the geochemical variability of the Green River petroleum. Previous geochemical studies of the Green River oils have found distinct populations of oils based on geochemical heterogeneities (Lillis et al., 2003). The GRA oils have high wax content, a carbon preferential index less than 1.10, and low β-carotane content (Fig. 2; Lillis et al., 2003). The GRA oils are the most common type and make up most of our oil samples and all of the tar sand samples ($n = 23$; Table 1). This clarifies that the tar sands are migrated and biodegraded deposits of the Green River oils. The GRB oils, of which we have a few samples ($n = 5$), are geochemically similar to gilsonite and generally have higher odd-carbon predominance (carbon preferential index greater than 1.2) and higher β-carotane content (Fig. 2; Lillis et al., 2003). Geochronology of these two subsets based on β-carotane content (Table 1) provides ages in

agreement with previous Re–Os geochronology (Isochrons 13 and 14 – Table 4; Fig. 4E and F), but does not provide distinct generation ages for these two subsets. This supports findings that suggest that the Green River petroleum is geochemically more complex than two end-member petroleum types reflecting complex spatial variation in the source rock (Ruble et al., 2001). This source rock variation is likely causing the large variation in Os_i and the main reason for producing high uncertainties in the Re–Os geochronology as discussed in previous studies (Selby et al., 2005; Selby and Creaser, 2005a; Finlay et al., 2011).

Without considering Os_i, the Re–Os geochronology derived from the Green River petroleum broadly agrees with previous basin models (Fouch et al., 1994; Ruble et al., 2001). However, the geochronology is hampered by mixing of oils generated at different times and from different stratigraphic intervals of the Green River Formation, and therefore containing variable Os_i as has been seen in previous studies (Selby et al., 2005; Selby and Creaser, 2005a,b; Lillis and Selby, 2013). When taking the Os_i variation into account the precision of Re–Os geochronology improves. Regardless, this study suggests that Re–Os geochronology can be applied to Type I lacustrine kerogen-derived petroleum including oils and tar sands. Both oils and tar sands have previously been successfully dated using Re–Os in marine petroleum systems (Selby and Creaser, 2005a; Finlay et al., 2011). This study therefore widens the capabilities of Re–Os petroleum geochronology beyond marine petroleum systems to lacustrine petroleum systems.

5.2. Os isotope oil to source rock correlation

5.2.1. Previous Green River petroleum system correlation studies

The source of the Green River petroleum system is known to be the Green River Formation. However this unit is over 3000 m thick in places and made up of several fluctuating-profundal organic-rich members interbedded with marginal fluvial sandstone deposits (Carroll and Bohacs, 2001; Keighley et al., 2003; Smith et al., 2008). Thus there is a large diversity of source rock facies available for petroleum generation and the exact units within the Green River Formation that are generating oil are ambiguous (Anders et al., 1992; Ruble et al., 2001). Oil-source rock correlation in these settings is complicated as multifaceted lacustrine facies can obscure maturity relationships usually distinguished by biomarkers (Ruble et al., 2001). However, several correlation studies have been attempted (Tissot et al., 1978; Anders et al., 1992; Hatcher et al., 1992; Ruble et al., 2001; Lillis et al., 2003). Source rock stratigraphy is said to control the composition of the oils and though the oil shales (e.g., the Mahogany zone) are organic-rich, they are not considered the dominant source rock. A classic correlation study using biomarkers linked the oils with the basal Green River Formation (Tissot et al., 1978). Comparison of oils derived from hydrous pyrolysis experiments on units from the Uinta Basin with natural oils also found the lower part of the Green River Formation, namely the black shale facies (part of the Douglas Creek Member), to be the main source of oils generated in the Uinta Basin (Ruble et al., 2001). Most studies agree on the lower part of the Green River Formation being the main source rock facies, but others do allude to the Mahogany zone having generated oil based on Rock–Eval generation models (Fouch et al., 1994). While the oils and therefore the tar sands are sourced from predominantly the lower part of the Green River Formation, gilsonite is sourced from the Mahogany zone based on infra-red spectra (Hunt et al., 1954), carbon isotopes (Schoell et al., 1994), and the observation that gilsonite veins are rooted in the Mahogany zone beds (Verbeek and Grout, 1992). Other solid bitumen deposits are associated with different intervals of the Green River Formation and the depositional environment is thought to play a significant role in controlling what type of bitumen is produced (Hunt, 1963). Gilsonite is predominantly derived from an algal source consistent with high lake levels and organic production associated with the Mahogany zone (Ruble et al., 1994; Schoell et al., 1994). Comparison of oil geochemical data with source rock geochemical data concluded that GRA petroleum phases (most abundant oils and tar sands) are most likely derived from the black shale facies of the lower Douglas Creek Member, whereas GRB petroleum phases (some oils and all gilsonite) are derived from the Mahogany zone (Lillis et al., 2003). However, even though these are still the main source units purported, it has also been suggested that the Green River petroleum reflects much more complex mixtures rather than two end-member types (Ruble et al., 2001).

5.2.2. Os isotope correlation

During petroleum generation the Os isotopic composition of the source is transferred to the produced petroleum (this study; Selby and Creaser, 2005a; Selby et al., 2005, 2007; Finlay et al., 2010, 2011, 2012; Rooney et al., 2012). This allows Os isotopes to be used as an oil-source correlation tool. Oil-source correlation using Os is based on the idea that the source $^{187}Os/^{188}Os$ composition at the time oil was generated (Os_g) will be transferred to the oil and hence the oils initial $^{187}Os/^{188}Os$ (Os_i) should have the same composition as Os_g. Due to the lack of clarity in the Re–Os oil generation results, the age of oil generation is taken from most recent models which suggest it began at ~25 Ma, which is overlapped by the Re–Os ages produced in this study (Ruble et al., 2001). This age also represents an average age of generation from previous models (Fouch et al., 1994) and therefore is suggested to be the most accurate estimate of oil generation. The Os_g and Os_i are back-calculated using the Re–Os isotopic compositions, the age of oil generation (25 Ma) and the ^{187}Re decay constant (Smoliar et al., 1996). The exact age of oil generation is not pertinent to oil-source correlation using Os, as the Os_g and Os_i will generally co-vary when calculated with changing oil generation ages and so correlation will still be accurate (see Fig. 5). Comparison of the Os_i of the petroleum to the Os_g of various source rocks gives the potential to fingerprint the source rock. For this study three Green River Formation source units from the Uinta Basin have been analysed as potential source rocks (Table 2; Cumming et al., 2012). Core M16 (Fig. 1) provides a section of the lower Douglas Creek Member at the southwest edge

of the basin. Core CW1 (Fig. 1) provides one section of the lower Douglas Creek Member in the central depocentre that has seen the most burial and one section of the Mahogany zone sampled from the central depocentre. The variation in the Os_g of the source is related to the depositional initial $^{187}Os/^{188}Os$ of the sample originating from the composition of Os in the lake water column, which is derived from weathering of the surrounding crust, the Re content of the sample and the time since deposition (Cumming et al., 2012). The large variation in Os_g of the source (1.43–2.13; Table 2) highlights that varying Os isotopic compositions are passed onto the petroleum and therefore make precise petroleum generation geochronology challenging. Certainly with generation moving upsection, the petroleum likely presents a mixture of sources that would account for the large variation seen in Os_i, particularly in the oils ($Os_i = 1.44–1.78$) and tar sands ($Os_i = 1.31–1.82$). The lower variation in the gilsonite ($Os_i = 1.55–1.70$) compared to the oils and tar sands, may reflect one source rather than a potential mixture of oils/sources for the oils and tar sands. This supports the idea that gilsonite was generated quickly from one source (Hunt, 1963; Verbeek and Grout, 1992). Solid bitumen deposits such as gilsonite have not been assessed using Re–Os before and the resultant effects on Re–Os systematics of the process of solidification of the gilsonite are not known (Hunt, 1963; Tetting, 1984). Bitumen found in the Polaris Mississippi Valley-type deposit was dated successfully using Re–Os (Selby et al., 2005), but this is interpreted to be a biodegraded residue of conventional crude oil (similar to the oil found in tar sands) rather than a solidified state (such as gilsonite).

In order to analyse the Os_i and Os_g, histograms have been plotted of all the values for the source rock and petroleum samples to deduce the modal values and link these to their respective sources, allowing the source rock to be identified. The spectrum seen on both histograms illustrates the variation in the source rocks and hence the variation in the Os_i of the petroleum that was generated. The source rocks show a majority of Os_g values around 1.6 and 1.7, with the petroleum's mode at 1.6 (Fig. 6). However, there are smaller data clusters at 1.4 and 1.5, with values at ~1.4 not accounted for by the source rocks. This suggests that the three sampled units do not fully represent the Green River Formation units that are generating petroleum in the Uinta Basin. When the petroleum is analysed separately as oils, tar sands, and gilsonite, and the source rocks are separated into Douglas Creek Member (M16), Douglas Creek Member (CW1) and Mahogany zone (CW1), a better appreciation of the Os composition of the sources and petroleum is gained (Fig. 6). The gilsonite and the Mahogany zone appear to dominate the 1.6 values in the two histograms, suggesting that correlation using $^{187}Os/^{188}Os$ supports the previously suggested notion that gilsonite is sourced from the Mahogany zone (Hunt et al., 1954; Verbeek and Grout, 1992; Ruble et al., 1994; Schoell et al., 1994; Lillis et al., 2003). In addition, the GRB oils have an Os_i value of predominantly ~1.6, similar to the gilsonite, suggesting that they are both sourced from the Mahogany zone as proposed by Lillis et al. (2003). This suggests that the Os correlation is supporting organic geochemical correlations

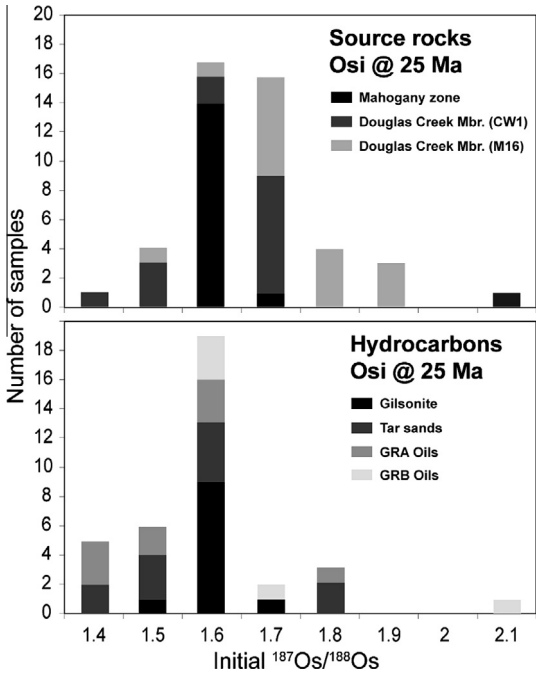

Fig. 6. Os_i histograms for the petroleum and source rocks calculated at 25 Ma. The different shades of grey (see key) show the different petroleum types and different source rocks analysed. This gives an impression of which petroleum phases were sourced from certain source rocks sampled.

using the biomarker β-carotane and odd-carbon predominance. The GRA oils and tar sands seem to dominate from 1.4 to 1.6. However, the other two source units dominate from 1.5 to 1.9, the Douglas Creek Member (M16), in particular, has values predominantly >1.7. This unit comes from the southwest corner of the basin where the units have not been buried sufficiently for oil generation, which is supported by the Os data suggesting that this unit has not generated any of the petroleum sampled for this study. This suggests that lateral variation within source units can also affect the Os isotope composition. The other units are derived from the central-northeast depocentre where most of the petroleum generation has occurred (Anders et al., 1992; Fouch et al., 1994). The exact source of the GRA oils and tar sands is not conclusive from this study, but it would seem both the Douglas Creek Member (CW1) and the Mahogany zone (CW1) are likely source units based on Os, or that the source may have originated in unsampled strata between these two units. Based on previous studies, the GRA oils and tar sands should be sourced from the lower part of the Green River Formation (Douglas Creek Member or black shale facies; Tissot et al., 1978; Fouch et al., 1994; Ruble et al., 2001; Lillis et al., 2003). However, they are geochemically complex rather than two end-member types and so the source rock may not be restricted to a specific interval. The Os data support this finding, therefore suggesting that Os isotopes do provide a valuable means for oil-source correlation. The Os isotope correlation tool may not be able to differentiate between complex lacustrine facies within the Green River Formation, but certainly

the Os isotope composition is passed from source to petroleum and can be used as a robust correlation tool, despite biodegradation and unusual mechanisms of formation of solid bitumen (e.g., gilsonite).

5.3. Hydrous pyrolysis insights into Re–Os systematics

5.3.1. Re–Os abundances and isotopic compositions of hydrous pyrolysis products

Hydrous pyrolysis has previously been used to assess Re and Os transfer to oils in Type II-S and Type III marine kerogens (Rooney et al., 2012). The findings from their study demonstrated that >95% of Re and Os remain within the extracted rock implying that thermal maturation at oil-generative levels does not result in significant transfer of Re and Os into liquid organic phases and that the majority of Re and Os are complexed within the kerogen fraction of an organic-rich rock. Additionally, they found only minor variations in $^{187}Re/^{188}Os$ and $^{187}Os/^{188}Os$ ratios in the original rock, recovered rock, and extracted rock from each experiment, suggesting that thermal maturation does not affect Re–Os systematics in organic-rich sediments of different maturities as seen in natural systems (Creaser et al., 2002; Kendall et al., 2004; Selby and Creaser, 2005b; Rooney et al., 2010). Our study further corroborates these findings; only minor discrepancies in Re and Os abundances are recorded in the original rock, recovered rock, and extracted rock (Table 7) which are most probably due to natural variations seen in the different aliquots being used for analysis. Our study also only sees <5% transfer of Re and Os into liquid organic phases from the source rock. The analysis of the extracted rock effectively represents analysis of the kerogen, because the soluble bitumen has been removed and the extracted rock contains only insoluble organic matter. Therefore, because the Re–Os digestion method preferentially digests organic matter, only the kerogen will be analysed (Selby and Creaser, 2003; Kendall et al., 2004; Rooney et al., 2011). The finding that $^{187}Re/^{188}Os$ and $^{187}Os/^{188}Os$ ratios in the original rock and extracted rock, and the recovered rock and extracted rock from each experiment (Table 8) show only variations that are within uncertainty of each other, provides evidence that Re and Os reside in the kerogen of a Type I lacustrine organic-rich rock and that maturation does not adversely affect the systematics and abundances of Re and Os in these source rock types. This allows us to conclude that Re–Os geochronology of Type I lacustrine kerogen is not adversely affected by petroleum maturation, just as is seen in marine kerogens (Creaser et al., 2002; Selby and Creaser, 2005a; Rooney et al., 2010, 2012; Cumming et al., 2012).

The experimental conditions for the hydrous pyrolysis experiments undertaken in this study are based on a previous study on the same samples where a series of experiments allowed peak-bitumen and peak-oil generation to be deduced (Ruble et al., 2001). These temperatures of 330 °C and 360 °C, respectively, were employed in this study to enable assessment of Re and Os transfer and systematics at peak-bitumen and peak-oil generation for the two different Green River source rocks. In this study we find that there is limited transfer of Re and Os to the free oil or bitumen during high temperature (360 °C) hydrous pyrolysis experiments and also that there is limited transfer to the free oil during the 330 °C experiment. This was also reported by Rooney et al. (2012) and it was suggested that the kinetic parameters fundamental for the transfer of Re and Os to oils are not achieved during hydrous pyrolysis experiments at the high temperatures and short durations employed. The peak-bitumen 330 °C experiments, however, do see transfer of Re and Os to the bitumen fraction. They contain ~2 orders of magnitude less Re and Os than the source rock, but roughly two orders of magnitude more than the bitumen in the 360 °C experiments and the free oils from both experiments (Table 7). Rooney et al. (2012) found that both Re and Os concentrations in bitumen increase with rising bitumen generation, until substantial oil generation occurs (>300 °C) when the bitumen is thermally decomposing to oil and/or pyrobitumen. Our study mimics this finding as in the peak-oil generation experiments (360 °C) there is limited Re and Os in the extracted bitumen. This suggests that the Re and Os in the bitumen could be assimilated into pyrobitumen by cross-linking reactions rather than transferring into the expelled oil during thermal cracking (Lewan, 1997; Rooney et al., 2012). This finding is also observed in V and Ni studies of hydrous pyrolysis products which found significant transfer to the bitumen, but only minor amounts to the oils. The proportions of V to Ni stay the same indicating no preferential transfer of one element to another, suggesting they are bound in similar compounds (Lewan, 1980).

Assessment of $^{187}Re/^{188}Os$ and $^{187}Os/^{188}Os$ ratios in the rocks and extracted bitumen allow the relative systematics of Re and Os transfer to be assessed (Table 8; Fig. 3). Because of negligible abundances in the free oil, these samples had large uncertainties (up to 100%) due to blank corrections and therefore are not reported. The $^{187}Re/^{188}Os$ ratios show slight variation from original rock to recovered rock in the 330 °C experiment, but the $^{187}Os/^{188}Os$ ratios remain similar throughout (330 °C and 360 °C), around 1.8 for the Mahogany zone rocks and 1.6 for the black shale facies rocks. This suggests no appreciable disturbance to Os isotopic compositions in the rocks. In the naturally occurring bitumen extracted from the original Mahogany zone rock, both $^{187}Re/^{188}Os$ and $^{187}Os/^{188}Os$ ratios are higher than the original rock (427.4–596.0 and 1.768–2.008, respectively), which is not observed for the black shale facies. Rooney et al. (2012) saw a large increase in the bitumen $^{187}Re/^{188}Os$ ratios (more than doubling) from the original rock and a slight increase in the $^{187}Os/^{188}Os$ ratios in hydrous pyrolysis experiments on the Phosphoria Formation. This was interpreted to be due to preferential transfer of Re over Os into the bitumen giving high $^{187}Re/^{188}Os$ ratios (Selby et al., 2005), which then allowed radiogenic in-growth of ^{187}Os over time. Due to the hydrous pyrolysis experiments being instantaneous on geological time scales, there is no radiogenic in-growth of ^{187}Os. The $^{187}Os/^{188}Os$ for the Mahogany zone natural bitumen show evidence of radiogenic in-growth of ^{187}Os, however in all other cases in the bitumen extracted from the original rock (black shale facies) and recovered rock (all 330 °C experiments), $^{187}Os/^{188}Os$ ratios all stay approximately the same at 1.8

(Mahogany zone) and 1.6 (black shale facies), with the $^{187}Re/^{188}Os$ values decreasing. This may suggest that the natural bitumen extracted from the black shale facies has been generated very recently and so behaves similarly to an 'instantaneous' hydrous pyrolysis experiment giving minimal in-growth of radiogenic ^{187}Os. This conclusion for the black shale facies coincides with the fact that the Green River Formation continues to have ongoing petroleum generation. Thus, it is certainly possible that the natural bitumen extracted from the original rocks have been generated relatively recently (Fouch et al., 1994; Ruble et al., 2001). In contrast, the Mahogany zone has a much higher TOC of 15.23 wt.% as opposed to 5.86 wt.% for the black shale facies (Table 6). It may be that variation in organic matter or levels of organic matter allowed the Mahogany zone to have generated minor amounts of bitumen prior to the black shale facies. As a result the incorporation of Re over Os into the Mahogany zone naturally generated bitumen permitted the analysed bitumen of this study to possess a more radiogenic $^{187}Os/^{188}Os$ composition.

The bitumen from the 360 °C experiments have much lower $^{187}Re/^{188}Os$ and $^{187}Os/^{188}Os$ values than the other experiments (Table 8). The uncertainties are very large on very low abundances and any interpretation is made with caution, but the nominal values may suggest Re–Os fractionation during bitumen-to-oil generation that has not gone to completion. The asphaltenes derived from the free oil in peak-oil generation (360 °C) experiments show an increase in $^{187}Re/^{188}Os$ values from the recovered rock and a minor decrease in the $^{187}Os/^{188}Os$ ratios in the Mahogany zone to 1.5, but stay the same at 1.6 for the black shale facies. The $^{187}Os/^{188}Os$ ratios are very stable throughout thermal maturation, with the only exception of the asphaltene of Mahogany zone free oil that reduces to 1.52 from 1.76. This may relate to the asphaltene extraction, as incomplete extractions have previously been suggested to affect the Re–Os systematics in asphaltenes derived from artificial experiments (Reisberg et al., 2008). It may also suggest the hydrous pyrolysis experiments on the Mahogany zone are not mimicking the natural environment as well as the black shale facies and that the difference in these two rock types is important for Re and Os transfer and fractionation. Overall, $^{187}Re/^{188}Os$ ratios tend to be decreasing in the bitumen relative to the original rock and then increasing in the asphaltene of the expelled oil, which suggests some variation in the relative transfer of Re. The reason for the decrease in $^{187}Re/^{188}Os$ ratios may be that Re is more tightly bound in a Type I kerogen (compared to Type II-S and Type III; Rooney et al., 2012) and less Re is transferred to the bitumen during generation as evidenced by the low values in the $^{187}Re/^{188}Os$ bitumen. However, when the free oil is generated, it is possible that there is enough thermal stress for Re to be transferred, hence the higher $^{187}Re/^{188}Os$ ratios in the asphaltene.

The hydrous pyrolysis experiments may not mimic natural transfer of the $^{187}Re/^{188}Os$ composition from source to oil, making assessment of natural fractionations challenging. Comparison with the data from the natural samples shows no consistent relationship between source and petroleum $^{187}Re/^{188}Os$ ratios. In this study the petroleum products generally have lower $^{187}Re/^{188}Os$ ratios (70.3–674.1) than the source rocks (98.6–1830.5). A study from the Western Canadian Oil Sands shows a range of $^{187}Re/^{188}Os$ ratios of 1028–1429 in oil from the tar sands whereas the source (the Gordondale Formation; as suggested by the study) has $^{187}Re/^{188}Os$ ratios of 550.4–1674 (Finlay et al., 2012). These data provide no solid conclusions for the relationship of transfer of $^{187}Re/^{188}Os$ ratios. As noted below, investigating the system using hydrous pyrolysis experiments has revealed that organic matter type may be one of the main controls on the transfer kinetics of Re and Os and therefore it is important that the location of Re and Os in kerogen be more fully understood.

The similarity of Os compositions throughout thermal maturation is also found in Type II-S and Type III kerogens (Rooney et al., 2012) and confirms that Os can be a very useful correlation tool from oil to source as suggested in previous studies (Selby and Creaser, 2005a; Selby et al., 2007; Finlay et al., 2011, 2012; Rooney et al., 2012). The slight variation in both the $^{187}Re/^{188}Os$ and $^{187}Os/^{188}Os$ in the Mahogany zone (Fig. 3) may suggest that the two source rocks contain different organic compounds where Re and Os are held, yielding different systematics, exemplified by their greatly different abundances of Re (24.61 and 3.88 ng/g for the Mahogany zone and black shale facies, respectively) and Os (0.337 and 0.161 ng/g for the Mahogany zone and black shale facies, respectively). The Mahogany zone and black shale facies are known to contain variation in their kerogen and were deposited under different conditions (Castle, 1990; Tuttle and Goldhaber, 1993; Ruble et al., 2001; Smith et al., 2008). The concentration of the precursors of the compounds responsible for chelating Re and Os may be different as a result of different depositional settings. Metal enrichment in sediments is a complex process where many variables are concerned, including sedimentation rate, type of organic matter, and depth of the oxic-anoxic transition (Lewan and Maynard, 1982; Selby et al., 2009; Rooney et al., 2012). The distinct chelating precursors of Re and Os may be responsible for the different Re–Os systematics seen in the two source rock samples and exemplifies the need to identify the compounds containing Re–Os in order to better interpret both source rock and oil geochronology. Variation in $^{187}Re/^{188}Os$ could potentially suggest transfer of Re and Os at different rates and so they may not be held in the same compounds as V and Ni, which transfer proportionally (Lewan, 1980).

5.3.2. Comparison with the natural Green River petroleum system

Comparison of Re and Os abundances of the natural Green River petroleum system with the products derived from the hydrous pyrolysis experiments is illustrated in Fig. 7. All of the samples from both natural and hydrous pyrolysis experiments plot along one trend. In the natural Green River petroleum system, there is a similar amount of variability in the Re and Os of the source as is seen in each of the derived petroleum phases. The gilsonite contains an order of magnitude less Re and Os than the source rocks, with the tar sands and asphaltenes extracted from the oils containing another order of magnitude less. The

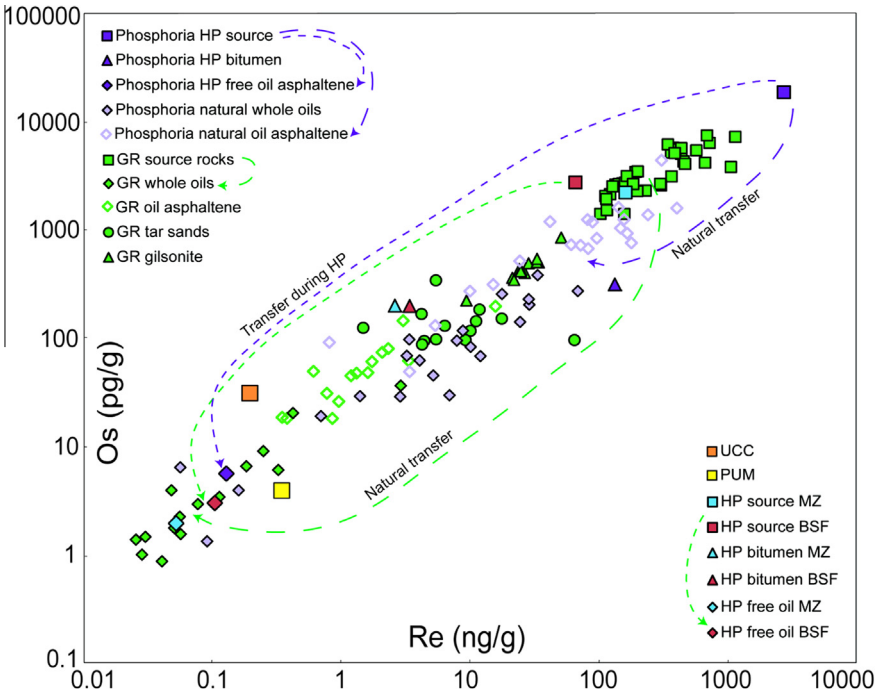

Fig. 7. Log–log Re and Os abundance graph for the Green River and Phosphoria natural and hydrous pyrolysis systems. The Phosphoria natural data are taken from Lillis and Selby (2013) and the hydrous pyrolysis data are taken from Rooney et al. (2012). The Re and Os abundances of the source rocks are calculated on a TOC basis so as to see relative transfer from kerogen to petroleum. The green arrows show approximate transfer from the source to the natural oils and the hydrous pyrolysis free oil for the Green River Formation. The purple arrows show approximate transfer from the source to the natural oil asphaltene and the hydrous pyrolysis free oil asphaltene for the Phosphoria Formation. Asphaltene is compared for the Phosphoria system as there are no values for the free oil derived from hydrous pyrolysis experiments as the abundances were too low to measure (Rooney et al., 2012). The figure shows that the Green River hydrous pyrolysis experiments mimic the natural system much better than the Phosphoria system, which would be even more exaggerated if data for the Phosphoria free oil could be compared. See key for sample details. GR = Green River; HP = hydrous pyrolysis; MZ = Mahogany zone; BSF = black shale facies; UCC = upper continental crust (Peucker-Ehrenbrink and Jahn, 2001); PUM = primitive upper mantle (Becker et al., 2006). (For interpretation of the references to color in this figure legend, the reader is referred to the web version of this article.)

whole-oil abundances (based on asphaltene content) are approximately 4 orders of magnitude less than the source rock. The whole-oil abundances are low because the asphaltene contents of these oils are generally very low (Table 1), in part because the majority of them show no biodegradation, which would normally enrich the asphaltene content, and because they are higher thermal maturity oils which decreases asphaltene contents (Milner et al., 1977). Thermal maturity of petroleum in the Uinta Basin has been assessed in terms of vitrinite reflectance equivalent, with gilsonite having values of 0.5% R_m, tar sands <0.8% R_m and oils generally from 0.7% to 1.3% R_m (Anders et al., 1992; Fouch et al., 1994). This shows that the oils are the most mature petroleum phase produced and is reflected in their low asphaltene contents (Evans et al., 1971; Milner et al., 1977). Higher maturity oils would also have lower levels of nitrogen–sulphur–oxygen compounds and porphyrins, which may explain the low Re and Os abundances as Re and Os have been suggested to be held in these compounds (Miller, 2004; Selby et al., 2007; Rooney et al., 2012). The petroleum phases with higher Re and Os abundances correlate with the higher asphaltene contents in the gilsonite and tar sands (Table 1), and also the GRB oils have higher Re and Os abundances and asphaltene than the GRA oils. The GRB oils are thought to have been sourced from the Mahogany zone, which would explain the lower maturity of the oils as the Mahogany zone is higher in the section and so the GRB oils must have been generated more recently than the GRA oils (Fouch et al., 1994; Ruble et al., 2001; Lillis et al., 2003). The Mahogany zone is also the most enriched source unit and so this suggests that Re and Os contents of the source directly affects how much is transferred to the petroleum. Because Re and Os are predominantly held within the asphaltene fraction of petroleum (Selby et al., 2007), the gilsonite and tar sands have higher Re and Os contents than the oils, most likely relative to their much higher asphaltene contents (Table 1). The gilsonite, like the GRB oils is said to be sourced from the Mahogany zone and with increased Re and Os content up to an order of magnitude more than the tar sands, may be related to the higher Re and Os contents of the source, again showing proportionality in transfer from source to petroleum.

There is limited transfer of Re and Os to expelled oils during experimental pyrolysis, a finding that has been noted in previous studies (Reisberg et al., 2008; Rooney et al., 2012). Our study coupled with these previous studies, suggest that this is the case for Type I lacustrine, Type II, Type II-S and Type III kerogens. This is an unexpected experimental artefact in that natural crude oils derived from all

these kerogen types contain substantial Re and Os (Woodland et al., 2001; Selby and Creaser, 2005a; Selby et al., 2007; Finlay et al., 2010, 2011; Lillis and Selby, 2013). However, when the Re and Os abundances of the hydrous pyrolysis products including the pyrolyzed source rocks, and the bitumen and free oil from the peak-bitumen and peak-oil experiments are plotted on Fig. 7, there is a correlation with the natural Green River petroleum system. The pyrolyzed source rocks have similar abundances to the range of source rocks sampled for analysis of the natural system, although are at the lower end of the scale. The Re and Os contents of the hydrous pyrolysis peak-bitumen generation are similar to the lower values for gilsonites and the higher contents for the tar sands. This may suggest that the gilsonite is a similar petroleum product to bitumen forming early at peak-bitumen formation rather than during oil generation. Gilsonite has previously been suggested as an unusual early expulsion product that is immature with thermal maturity equivalent to a vitrinite reflectance value of 0.5% R_m (Anders et al., 1992; Verbeek and Grout, 1992). The free oil from the peak-oil hydrous pyrolysis experiments, interestingly, contains similar Re–Os abundances to the lower values for whole oils from the natural Green River petroleum system. This again reflects proportionality in transfer from the lower abundance sources to the free oil. These results suggest that the hydrous pyrolysis experiments are producing Re and Os abundances similar to the natural system and so may in fact be mimicking natural Re and Os transfer in a Type I lacustrine kerogen, unlike previous hydrous pyrolysis experiments (Rooney et al., 2012). This may suggest that the kinetics achieved during hydrous pyrolysis of a Type I lacustrine kerogen allow Re and Os transfer and fractionation to occur in a similar fashion to natural Re and Os transfer.

In order to compare this with another system that has been assessed from a natural generation and hydrous pyrolysis generation perspective, data for the Phosphoria Formation petroleum system has been plotted on Fig. 7. The hydrous pyrolysis data are taken from Rooney et al. (2012) and the natural oil data are taken from Lillis and Selby (2013). The Phosphoria petroleum system shows a trend similar to the Green River petroleum system although with slightly more scatter. The Phosphoria source rock has Re and Os contents an order of magnitude higher than the Green River Formation. The natural oil asphaltenes are only an order of magnitude less than the Phosphoria source rock and the whole oils (based on asphaltene contents) are only again an order of magnitude less than the asphaltenes. This signifies that the Phosphoria whole oils are only two orders of magnitude less enriched in Re and Os than the source, compared to 4 orders of magnitude less for the Green River petroleum system. This shows that the higher abundance source is delivering higher levels of Re and Os to the oils and suggests that the different kerogen types may require different kinetics for transfer of Re and Os. Therefore the higher asphaltene contents of the oils (Lillis and Selby, 2013) means that they are proportionally more enriched than the Green River natural oils, suggesting that source abundance and asphaltene content are controlling factors in Re and Os enrichment of petroleum. The products from the Phosphoria hydrous pyrolysis experiments show that the peak-bitumen Re and Os contents are only slightly higher than the whole oils, compared to over an order of magnitude higher in the Green River Formation experiments. In stark contrast to the Green River Formation hydrous pyrolysis experiments, the Re and Os contents of the Phosphoria asphaltene from the free oil at peak-oil generation has 1–2 orders of magnitude less Re and Os than most of the natural Phosphoria whole oils. The whole-oil values for the free oil cannot be calculated as the asphaltene contents are not known and the whole free oil contained no measurable Re or Os. The hydrous pyrolysis asphaltene is almost 3 orders of magnitude lower than the natural oil asphaltenes in the Phosphoria system. This indicates completely different systematics in the Phosphoria system compared to the Green River petroleum system and suggests that kerogen type may play an important role in Re and Os transfer to petroleum. It certainly indicates that the transfer seen in the Green River Formation hydrous pyrolysis experiments may be mimicking the kinetics achieved in the natural system, whereas the kinetics in the Phosphoria Formation hydrous pyrolysis experiments do not (Rooney et al., 2012). Although kerogen cracking may be different between the two types and certainly affects Re and Os transfer during hydrous pyrolysis experiments, the Re–Os isotopic compositions remain similar throughout both sets of experiments.

The similarity in $^{187}Os/^{188}Os$ compositions of the source rock and produced organic phases in the hydrous pyrolysis experiments provides strong support for $^{187}Os/^{188}Os$ compositions as an oil-source correlation tool as has been employed in the natural Green River petroleum system for this study (above 5.2.2). In the hydrous pyrolysis experiments we see that the Mahogany zone source rock has an $^{187}Os/^{188}Os$ composition of ~1.8 as does the produced bitumen (Fig. 3). In the black shale facies the $^{187}Os/^{188}Os$ composition is ~1.6, the same as the produced bitumen and asphaltene from the free oil (Fig. 3). The majority of Os compositions of the natural oils and sources are ~1.6, which is comparable to the hydrous pyrolysis experimental products. The similarity in compositions through the hydrous pyrolysis experiments shows that there is direct transfer of the $^{187}Os/^{188}Os$ compositions during oil generation and validates the assumption that generated petroleum will have the same Os isotopic composition as the source at the time the petroleum was generated (this study; Rooney et al., 2012). There is strong evidence that the Os correlation tool is robust and suggests that this tool can be successfully applied to multiple petroleum system types and with different petroleum phases (Selby and Creaser, 2005a,b; Selby et al., 2005; Finlay et al., 2012).

6. CONCLUSIONS

This study presents Re–Os geochronology of various petroleum phases (oils, tar sands and gilsonite) derived from the Green River petroleum system that broadly agrees with previous petroleum generation basin models (Ruble et al., 2001). The results provide valuable insight into Re–Os petroleum generation geochronology of variable petroleum phases derived from lacustrine Type I kerogen,

illustrating that the Re–Os systematics are similar to those in marine petroleum systems (Selby et al., 2005, 2007; Selby and Creaser, 2005a; Selby et al., 2007; Finlay et al., 2011). However, the young age of the Green River petroleum system and long duration of oil generation make interpretation of Re–Os geochronology challenging. The large uncertainties (Table 4) produced for the petroleum Re–Os geochronology are derived from variation in the initial Os isotopic composition (Os_i.) of the Green River source rocks, which is transferred to the petroleum during generation. This variation is due to it being a petroleum system with multiple generation events and multiple source units (within the ~3000-m thick Green River Formation; Fouch et al., 1994; Ruble et al., 2001), therefore creating a mixture of Os isotope compositions in the produced petroleum hampering Re–Os geochronology. When separating the samples based on Os_i, the precision of the geochronology increases as well as when separating them based on bulk geochemical properties. The Green River oils have very low Re and Os abundances that hampers precise determinations of isotope compositions, reducing the precision of Re–Os geochronology. Fundamental aspects of precise Re–Os petroleum geochronology therefore require samples with abundances that allow accurate analysis and also for samples to be sourced from a discrete source unit that would transfer similar Os isotopic compositions.

Oil-to-source fingerprinting using Os isotopes is also effective in lacustrine systems exemplified by this study. Wide variations in geochemical compositions due to rapid changes in depositional settings in time and space affect the Os correlation system as has been seen when using other geochemical correlation parameters in lacustrine systems. However, the Os_i value of ~1.6 for the gilsonite and GRB oils deduces their source as the Mahogany zone which has an Os_g value of ~1.6. The Os_i also suggests the lower Douglas Creek Member (CW1) as the most probable source of the GRA oils and tar sands. These Os isotope fingerprinting results are consistent with previous correlation studies in the Green River petroleum system. The Douglas Creek Member from the M16 core has Os_i higher than all the petroleum phases (>1.7) and as it is from an area that is not buried sufficiently for oil generation, it is likely that this unit has not generated oil. These results illustrate the ability of Os isotopes to delineate the spatial variations within a petroleum system.

Hydrous pyrolysis experiments on the Green River Formation source rocks show that Re and Os transfer mimics the natural system unlike a previous study on the Phosphoria Formation (Rooney et al., 2012). This transfer from source to bitumen to oil does not affect source rock Re–Os systematics or Os isotopic compositions. This confirms that Os isotope compositions are transferred intact from source to petroleum during petroleum generation and can be used as a powerful correlation tool. In addition, these experiments further confirm that Re–Os systematics in source rocks are not adversely affected by petroleum maturation.

The comparison between the Phosphoria Formation and Green River Formation hydrous pyrolysis experiments imply that different kinetics are needed for Re and Os transfer from variable source rock kerogen (e.g., Type I vs. II vs. III) to an oil, demonstrating a need to understand the chelating sites of Re and Os within organic matter. Overall this study illustrates that the Re–Os petroleum geochronometer and Os isotope fingerprinting tools can be used on a wide range of petroleum phases sourced from variable kerogen types. Furthermore, hydrous pyrolysis experiments corroborate the findings from the natural system giving much stronger support for these tools.

ACKNOWLEDGEMENTS

This research was funded by a Lundin Petroleum CeREES Ph.D. scholarship and an AAPG Gustavus E. Archie Memorial International Grant awarded to V.M.C. The USGS and UCRC are thanked for providing petroleum samples. Tim Ruble is thanked for providing gilsonite samples and advice on sampling strategy. Andrew Rupke at the Utah Geological Survey is thanked for help with location of tar sands in the field. The USGS laboratory staff (Zach Lowry) are thanked for help with analyses. Michelle Tuttle is thanked for help with core logs and sample information. Alan Rooney is thanked for logistical assistance and sample collection in the field. Robert Dias and Dave Ferderer, Katz Suzuki, and an anonymous reviewer are thanked for helpful reviews of the manuscript. Any use of trade, firm, or product names is for descriptive purposes only and does not imply endorsement by the U.S. Government.

REFERENCES

Anders D. E., Palacas J. G. and Johnson R. C. (1992) Thermal maturity of rocks and hydrocarbon deposits, Uinta Basin, Utah. In *Hydrocarbon and Mineral Resources of the Uinta Basin Utah and Colorado*, vol. 20 (eds. T. D. Fouch, V. F. Nuccio and T. C. Chidsey). Utah Geological Association Guidebook, pp. 53–76.

Becker H., Horan M. F., Walker R. J., Gao S., Lorand J. P. and Rudnick R. L. (2006) Highly siderophile element composition of the Earth's primitive upper mantle: constraints from new data on peridotite massifs and xenoliths. *Geochim. Cosmochim. Acta* **70**, 4528–4550.

Bohacs K. M., Carroll A. R., Neal J. E. and Mankiewicz P. J. (2000) Lake-basin type, source potential, and hydrocarbon character: an integrated sequence-stratigraphic–geochemical framework. *Lake Basins through Space and Time: American Association of Petroleum Geologists, Studies in Geology* **46**, 3–34.

Bradley W. H. (1931) Origin and microfossils of the oil shale of the Green River formation of Colorado and Utah. U.S. Geological Survey, Prof. Pap. 168, 58p.

Bredehoeft J., Wesley J. and Fouch T. (1994) Simulations of the origin of fluid pressure, fracture generation, and the movement of fluids in the Uinta Basin, Utah. *AAPG Bull.* **78**, 1729–1747.

Carroll A. R. and Bohacs K. M. (1999) Stratigraphic classification of ancient lakes: balancing tectonic and climatic controls. *Geology* **27**, 99–102.

Carroll A. R. and Bohacs K. M. (2001) Lake-type controls on petroleum source rock potential in nonmarine basins. *AAPG Bull.* **85**, 1033–1053.

Cashion W. B. (1967) *Geology and fuel resources of the Green River Formation, southeastern Uinta basin, Utah and Colorado*. US, Geological Survey, Prof. Pap, 548.

Castle J. W. (1990) Sedimentation in Eocene Lake Uinta (Lower Green River Formation), northeastern Uinta Basin, Utah. In

Lacustrine basin exploration-case studies and modern analogs: AAPG Memoir, vol. 50 (ed. B. J. Katz). pp. 243–263.

Cohen A. S., Coe A. L., Bartlett J. M. and Hawkesworth C. J. (1999) Precise Re–Os ages of organic-rich mudrocks and the Os isotope composition of Jurassic seawater. *Earth Planet. Sci. Lett.* **167**, 159–173.

Creaser R. A., Papanastassiou D. A. and Wasserburg G. J. (1991) Negative thermal ion mass spectrometry of osmium, rhenium and iridium. *Geochim. Cosmochim. Acta* **55**, 397–401.

Creaser R. A., Sannigrahi P., Chacko T. and Selby D. (2002) Further evaluation of the Re–Os geochronometer in organic-rich sedimentary rocks: a test of hydrocarbon maturation effects in the Exshaw Formation, Western Canada Sedimentary Basin. *Geochim. Cosmochim. Acta* **66**, 3441–3452.

Cumming V. M., Selby D. and Lillis P. G. (2012) Re–Os geochronology of the lacustrine Green River Formation: Insights into direct depositional dating of lacustrine successions, Re–Os systematics and paleocontinental weathering. *Earth Planet. Sci. Lett.* **359–360**, 194–205.

Du Vivier A. D. C., Selby D., Sageman B. B., Jarvis I., Gröcke D. R. and Voigt S. (2014) Marine $^{187}Os/^{188}Os$ isotope stratigraphy reveals the interaction of volcanism and ocean circulation during Oceanic Anoxic Event 2. *Earth Planet. Sci. Lett.* **389**, 23–33.

Dyni J. R. (2006) Geology and Resources of Some World Oil-Shale Deposits. U.S. Geological Survey Scientific Investigations Report 2005–5294.

Evans C. R., Rogers M. A. and Bailey N. J. L. (1971) Evolution and alteration of petroleum in western Canada. *Chem. Geol.* **8**, 147–170.

Finlay A. J., Selby D. and Osborne M. J. (2011) Re–Os geochronology and fingerprinting of United Kingdom Atlantic margin oil: temporal implications for regional petroleum systems. *Geology* **39**, 475–478.

Finlay A. J., Selby D. and Osborne M. J. (2012) Petroleum source rock identification of United Kingdom Atlantic Margin oil fields and the Western Canadian Oil Sands using platinum, palladium, osmium and rhenium: implications for global petroleum systems. *Earth Planet. Sci. Lett.* **313–314**, 95–104.

Finlay A. J., Selby D., Osborne M. J. and Finucane D. (2010) Fault-charged mantle-fluid contamination of United Kingdom North Sea oils: insights from Re–Os isotopes. *Geology* **38**, 979–982.

Fouch T. D., Nuccio V., Anders D., Rice D., Pitman J. and Mast R. (1994) Green River (!) petroleum system, Uinta Basin, Utah, USA. *AAPG Mem.* **60**, 399–421.

Gramlich J. W., Murphy T. J., Garner E. L. and Shields W. R. (1973) Absolute isotopic abundance ratio and atomic weight of a reference sample of rhenium. *J. Res. Natl. Bur. Stand.* **77A**, 691–698.

Hatcher H. J., Meuzelaar H. L. C. and Urban D. T. (1992) A comparison of biomarkers in gilsonite, oil shale, tar sand and petroleum from Threemile Canyon and adjacent areas in the Uinta Basin, Utah. In *Hydrocarbon and Mineral Resources of the Uinta basin, Utah and Colorado*, vol. 20 (eds. T. D. Fouch, V. F. Nuccio and T. C. Chidsey). Utah Geological Association Guidebook, pp. 271–287.

Higley D. K., Lewan M. D., Roberts L. N. R. and Henry M. (2009) Timing and petroleum sources for the Lower Cretaceous Mannville Group oil sands of northern Alberta based on 4-D modeling. *AAPG Bull.* **93**, 203–230.

Hindle A. D. (1997) Petroleum migration pathways and charge concentration: a three-dimensional model. *AAPG Bull.* **81**, 1451–1481.

Hunt J. M. (1963) Composition and origin of the Uinta Basin bitumens. In *The oil and Gas Possibilities of Utah, re-evaluated*, vol. 54 (ed. A. L. Crawford). Utah Geological and Mineralogical Survey Bulletin, pp. 249–276.

Hunt J. M., Stewart F. and Dickey P. A. (1954) Origin of hydrocarbons of Uinta basin, Utah. *AAPG Bull.* **38**, 1671–1698.

Johnson S. Y. (1992) Phanerozoic evolution of sedimentary basins in the Uinta-Piceance Basin region, northwestern Colorado and northeastern Utah. U.S. Geological Survey Bulletin 1787-FF.

Katz B. J. (1995) The Green River Shale: an Eocene carbonate lacustrine source rock. In *Petroleum Source Rocks* (ed. B. J. Katz). Springer-Verlag, pp. 309–324.

Keighley D., Flint S., Howell J. and Moscariello A. (2003) Sequence stratigraphy in lacustrine basins: a model for part of the Green River Formation (Eocene), Southwest Uinta Basin, Utah, USA. *J. Sediment. Res.* **73**, 987–1006.

Kendall B., Creaser R. A. and Selby D. (2009) $^{187}Re–^{187}Os$ geochronology of Precambrian organic-rich sedimentary rocks. *Geol. Soc. Lond., Spec. Publ.* **326**, 85–107.

Kendall B. S., Creaser R. A., Ross G. M. and Selby D. (2004) Constraints on the timing of Marinoan "Snowball Earth" glaciation by Re-187–Os-187 dating of a Neoproterozoic, post-glacial black shale in Western Canada. *Earth Planet. Sci. Lett.* **222**, 729–740.

Klemme H. and Ulmishek G. F. (1991) Effective petroleum source rocks of the world: stratigraphic distribution and controlling depositional factors (1). *AAPG Bull.* **75**, 1809–1851.

Lewan M. (1985) Evaluation of petroleum generation by hydrous pyrolysis experimentation. *Philos. Trans. R. Soc. Lond. Ser. A* **315**, 123–134.

Lewan M. D. (1980) Geochemistry of vanadium and nickel in organic matter of sedimentary rocks. Ph. D. thesis, University of Cincinnati.

Lewan M. D. (1997) Experiments on the role of water in petroleum formation. *Geochim. Cosmochim. Acta* **61**, 3691–3723.

Lewan M. D. and Maynard J. B. (1982) Factors controlling enrichment of vanadium and nickel in the bitumen of organic sedimentary rocks. *Geochim. Cosmochim. Acta* **46**, 2547–2560.

Lewan M. D. and Roy S. (2011) Role of water in hydrocarbon generation from Type-I kerogen in Mahogany oil shale of the Green River Formation. *Org. Geochem.* **42**, 31–41.

Lewan M. D. and Ruble T. E. (2002) Comparison of petroleum generation kinetics by isothermal hydrous and nonisothermal open-system pyrolysis. *Org. Geochem.* **33**, 1457–1475.

Lillis P. G. and Selby D. (2013) Evaluation of the rhenium–osmium geochronometer in the Phosphoria petroleum system, Bighorn Basin of Wyoming and Montana, USA. *Geochim. Cosmochim.* **118**, 312–330.

Lillis P. G., Warden A. and King J. D. (2003) Petroleum systems of the Uinta and Piceance Basins— geochemical characteristics of oil types, Chapter 3. In *Petroleum Systems and Geologic Assessment of Oil and Gas in the Uinta-Piceance Province, Utah and Colorado*. U.S. Geological Survey Digital Data Series DDS-69-B, 25p.

Ludwig K. (2008) Isoplot version 4.15: a geochronological toolkit for Microsoft Excel. Berkeley Geochronology Center, Special, Publication No. 4.

Ludwig K. R. (1980) Calculation of uncertainties of U–Pb isotope data. *Earth Planet. Sci. Lett.* **46**, 212–220.

Miller C. A. (2004) Re–Os dating of algal laminites: reduction-enrichment of metals in the sedimentary environment and evidence for new geoporphyrins. Ph.D. thesis, University of Saskatchewan.

Milner C. W. D., Rogers M. A. and Evans C. R. (1977) Petroleum transformations in reservoirs. *J. Geochem. Explor.* **7**, 101–153.

Nowell G. M., Luguet A., Pearson D. G. and Horstwood M. S. A. (2008) Precise and accurate $^{186}Os/^{188}Os$ and $^{187}Os/^{188}Os$ measurements by multi-collector plasma ionisation mass spectrometry (MC-ICP-MS) part I: Solution analyses. *Chem. Geol.* **248**, 363–393.

Peters K. E., Walters C. and Moldowan J. (2005) *The Biomarker Guide*, second ed. Cambridge University Press, UK, 1155p.

Peucker-Ehrenbrink B. and Jahn B. (2001) Rhenium–osmium isotope systematics and platinum group element concentrations: loess and the upper continental crust. *Geochem. Geophys. Geosyst.* **2**, 22.

Picard M. D. (1957) Red wash-walker hollow field, stratigraphic trap, Eastern Uinta Basin, Utah. *AAPG Bull.* **41**, 923–936.

Pietras J. T. and Carroll A. R. (2006) High-resolution stratigraphy of an underfilled lake basin: Wilkins Peak Member, Eocene Green River Formation, Wyoming, USA. *J. Sediment. Res.* **76**, 1197–1214.

Reisberg L., Michels R. and Hautevelle Y. (2008) Re/Os fractionation during generation and evolution of hydrocarbons. *Geochim. Cosmochim. Acta* **Suppl. 72**, 786.

Remy R. R. (1992) Stratigraphy of the Eocene Part of the Green River Formation in the South-Central Part of the Uinta Basin, Utah. U.S. Geological Survey Bulletin 1787-BB.

Rooney A. D., Chew D. M. and Selby D. (2011) Re–Os geochronology of the Neoproterozoic-Cambrian Dalradian Supergroup of Scotland and Ireland: Implications for Neoproterozoic stratigraphy, glaciations and Re–Os systematics. *Precambr. Res.* **185**, 202–214.

Rooney A. D., Selby D., Houzay J.-P. and Renne P. R. (2010) Re–Os geochronology of a Mesoproterozoic sedimentary succession, Taoudeni basin, Mauritania: Implications for basin-wide correlations and Re–Os organic-rich sediments systematics. *Earth Planet. Sci. Lett.* **289**, 486–496.

Rooney A. D., Selby D., Lewan M. D., Lillis P. G. and Houzay J.-P. (2012) Evaluating Re–Os systematics in organic-rich sedimentary rocks in response to petroleum generation using hydrous pyrolysis experiments. *Geochim. Cosmochim. Acta* **77**, 275–291.

Ruble T. and Philp R. (1991) Organic geochemical characterization of native bitumens from the Uinta Basin, Utah, USA. In *Organic Geochemistry: Advances and Applications in the Natural Environment* (ed. D. A. C. Manning). Manchester University Press, New York, pp. 97–99.

Ruble T. E., Bakel A. J. and Philp R. P. (1994) Compound-specific isotopic variability in Uinta Basin native bitumens – paleoenvironmental implications. *Org. Geochem.* **21**, 661–671.

Ruble T. E., Lewan M. D. and Philp R. P. (2001) New insights on the Green River Petroleum System in the Uinta Basin from hydrous pyrolysis experiments. *AAPG Bull.* **85**, 1333–1371.

Schoell M., Hwang R. J., Carlson R. M. K. and Welton J. E. (1994) Carbon isotopic composition of individual biomarkers in gilsonites (Utah). *Org. Geochem.* **21**, 673–683.

Scotchman I. C., Carr A. D. and Parnell J. (2006) Hydrocarbon generation modelling in a multiple rifted and volcanic basin: a case study in the Foinaven Sub-basin, Faroe-Shetland Basin, UK Atlantic margin. *Scott. J. Geol.* **42**, 1–19.

Selby D. and Creaser R. A. (2003) Re–Os geochronology of organic rich sediments: an evaluation of organic matter analysis methods. *Chem. Geol.* **200**, 225–240.

Selby D. and Creaser R. A. (2005a) Direct radiometric dating of hydrocarbon deposits using rhenium–osmium isotopes. *Science* **308**, 1293–1295.

Selby D. and Creaser R. A. (2005b) Direct radiometric dating of the Devonian–Mississippian time-scale boundary using the Re–Os black shale geochronometer. *Geology* **33**, 545–548.

Selby D., Creaser R. A., Dewing K. and Fowler M. (2005) Evaluation of bitumen as a Re-187–Os-187 geochronometer for hydrocarbon maturation and migration: a test case from the Polaris MVT deposit, Canada. *Earth Planet. Sci. Lett.* **235**, 1–15.

Selby D., Creaser R. A. and Fowler M. G. (2007) Re–Os elemental and isotopic systematics in crude oils. *Geochim. Cosmochim. Acta* **71**, 378–386.

Selby D., Mutterlose J. and Condon D. J. (2009) U–Pb and Re–Os geochronology of the Aptian/Albian and Cenomanian/Turonian stage boundaries: Implications for timescale calibration, osmium isotope seawater composition and Re–Os systematics in organic-rich sediments. *Chem. Geol.* **265**, 394–409.

Smith M. E., Carroll A. R. and Singer B. S. (2008) Synoptic reconstruction of a major ancient lake system: Eocene Green River Formation, western United States. *Geol. Soc. Am. Bull.* **120**, 54–84.

Smith M. E., Chamberlain K. R., Singer B. S. and Carroll A. R. (2010) Eocene clocks agree: Coeval $^{40}Ar/^{39}Ar$, U–Pb, and astronomical ages from the Green River Formation. *Geology* **38**, 527–530.

Smoliar M. I., Walker R. J. and Morgan J. W. (1996) Re–Os isotope constraints on the age of Group IIA, IIIA, IVA, and IVB iron meteorites. *Science* **271**, 1099–1102.

Sweeney J., Burnham A. and Braun R. (1987) A model of hydrocarbon generation from type I kerogen: application to Uinta basin, Utah. *AAPG Bull.* **71**, 967–985.

Tetting T. N. (1984) Origin of gilsonite fractures in the Uinta Basin, Utah. *AAPG Bull.* **68**, 951–952.

Tissot B., Deroo G. and Hood A. (1978) Geochemical study of the Uinta Basin: formation of petroleum from the Green River formation. *Geochim. Cosmochim. Acta* **42**, 1469–1485.

Tuttle M. L. and Goldhaber M. B. (1993) Sedimentary sulfur geochemistry of the Paleogene Green River Formation, western USA: implications for interpreting depositional and diagenetic processes in saline alkaline lakes. *Geochim. Cosmochim. Acta* **57**, 3023–3039.

Vandenbroucke M. and Largeau C. (2007) Kerogen origin, evolution and structure. *Org. Geochem.* **38**, 719–833.

Verbeek E. R. and Grout M. A. (1992) Structural evolution of gilsonite dikes, eastern Uinta Basin, Utah. U.S. Geological Survey Bulletin 1787-HH.

Völkening J., Walczyk T. G. and Heumann K. (1991) Osmium isotope ratio determinations by negative thermal ionization mass spectrometry. *Int. J. Mass Spectrom. Ion Processes* **105**, 147–159.

Walczyk T., Hebeda E. and Heumann K. (1991) Osmium isotope ratio measurements by negative thermal ionization mass spectrometry (NTI-MS). *Fresenius J. Anal. Chem.* **341**, 537–541.

Woodland S., Ottley C., Pearson D. and Swarbrick R. (2001) Microwave digestion of oils for analysis of platinum group and rare earth elements by ICP-MS. *Spec. Publ. – R. Soc. Chem.* **267**, 17–24.

Xu G. P., Hannah J. L., Stein H. J., Bingen B., Yang G., Zimmerman A., Weitschat W., Mork A. and Weiss H. M. (2009) Re–Os geochronology of Arctic black shales to evaluate the Anisian–Ladinian boundary and global faunal correlations. *Earth Planet. Sci. Lett.* **288**, 581–587.

York D. (1969) Least-squares fitting of a straight line with correlated errors. *Earth Planet. Sci. Lett.* **5**, 320–324.

Associate editor: Marc Norman